NACA RM A53J26

NACA

RESEARCH MEMORANDUM

THE USE OF A LEADING-EDGE AREA-SUCTION FLAP TO DELAY SEPARATION OF AIR FLOW FROM THE LEADING EDGE OF A 35° SWEPTBACK WING

By Curt A. Holzhauser and Robert K. Martin

Ames Aeronautical Laboratory
Moffett Field, Calif.

NATIONAL ADVISORY COMMITTEE
FOR AERONAUTICS
WASHINGTON

December 10, 1953
Declassified October 18, 1956

NATIONAL ADVISORY COMMITTEE FOR AERONAUTICS

RESEARCH MEMORANDUM

THE USE OF A LEADING-EDGE AREA-SUCTION FLAP TO DELAY SEPARATION OF AIR FLOW FROM THE LEADING EDGE OF A 35° SWEPTBACK WING

By Curt A. Holzhauser and Robert K. Martin

SUMMARY

An investigation was conducted on a 35° swept-wing model to determine the aerodynamic characteristics and suction requirements of a model having a leading-edge area-suction flap deflected 40°. These characteristics and suction requirements were compared with those reported in NACA RM A53E06 for the same model having leading-edge area suction (area suction applied to the unflapped leading edge). The aerodynamic characteristics (including pressure distributions) and suction requirements of the leading-edge area-suction flap were measured throughout a large angle-of-attack range for several extents and locations of the porous area near the highly curved surface formed when the leading-edge flap was deflected. The majority of the tests were made with a 40°, full-span, leading-edge, area-suction flap used in conjunction with a 55° trailing-edge area-suction flap. Tests were also run with an undeflected trailing-edge flap and with partial-span area suction on a full-span and on a partial-span leading-edge flap. The aerodynamic characteristics and suction requirements were measured for free-stream velocities varying from 112 to 166 feet per second.

Comparison of the results of the present investigation with those obtained for leading-edge area suction showed that comparable delays in air-flow separation from the leading edge of the wing were obtained with the 40° leading-edge area-suction flap, and that the power required for a given lift coefficient was only about one-tenth of that required for leading-edge area suction. This large reduction in power resulted from the lower flow coefficients and less negative suction pressure coefficients, each being about one-third of those required for leading-edge area suction.

It was found that air-flow separation from the leading edge of the wing was delayed with a full-span, leading-edge, area-suction flap (40°) from an angle of attack of 13° to 25° (from a lift coefficient of 1.60

to 2.27 when used with a 55° trailing-edge area-suction flap) by using a flow coefficient of 0.0006 and 23 horsepower (including duct and pump losses) at a free-stream velocity of 149 feet per second. The air-flow separation could be delayed to 29° angle of attack by approximately doubling the flow coefficient and suction pressure coefficient. It was found that the flow coefficient and plenum-chamber pressure coefficient were not affected by free-stream velocity, and, therefore, the suction power required for a given lift coefficient varied approximately with the cube of the free-stream velocity within the range tested.

Deflecting the leading-edge flap did not affect the lift increment provided by the trailing-edge area-suction flap. However, the suction requirements of the leading-edge flap for a given lift coefficient were reduced by deflecting the trailing-edge flap.

No large improvements in the pitching-moment characteristics at the maximum lift coefficient were obtained by applying partial-span area suction to the full-span or partial-span leading-edge flap. However, a large reduction in the maximum lift coefficient was incurred by applying partial-span suction rather than full-span suction.

INTRODUCTION

The current trend in the design of high-speed aircraft toward larger sweep angles and thinner airfoil sections makes it increasingly difficult to attain a high lift coefficient without air-flow separation. This air-flow separation frequently occurs from the leading edge of the wing at a relatively low angle of attack, and, as a consequence, the airplane can have undesirable pitching-moment characteristics, a reduced maximum lift coefficient, and increased drag at the higher lift coefficients. Air-flow separation from the leading edge has been effectively delayed to higher angles of attack by controlling the boundary layer with the application of area suction near the leading edge of the wing (refs. 1 to 5). The pumping power required for applications of this method to an airplane was considered to be high, primarily because of the high negative surface pressure coefficients near the leading edge of the wing.

Air-flow separation from the leading edge of a wing can also be delayed by deflecting a plain leading-edge flap (refs. 6 and 7). However, in order to delay the leading-edge flow separation to as high an angle of attack as with leading-edge area suction, the flap deflection would be so large that the flow would separate initially from the highly curved upper surface formed by the deflected flap (this curved surface is hereinafter referred to as the "knee"). In view of the results obtained with the NACA trailing-edge area-suction flap (ref. 1), it was reasoned that air-flow separation from the knee of a highly deflected

leading-edge flap could be delayed by applying area suction at the knee. Further, the external pressure coefficients at the knee of the deflected leading-edge flap would be much less negative than at the leading edge of the plain wing (i.e., the undeflected leading-edge flap) at the same angle of attack (ref. 6 or 7), and, consequently, less power should be required.

Because of the reductions in power indicated to be possible, an investigation was undertaken in the Ames 40- by 80-foot wind tunnel to obtain the aerodynamic characteristics and suction requirements of a model having a leading-edge area-suction flap in order to make a comparison with those of a model having leading-edge area suction. In order that a direct comparison of the two applications of area suction could be made, the 35° swept-wing model tested in references 1 and 2 was used. The present investigation was made with a deflected trailing-edge flap (the NACA trailing-edge area-suction flap (55°) discussed in ref. 1) and an undeflected trailing-edge flap. A limited study was also made to ascertain the changes in the pitching moment near the maximum lift coefficient that resulted from using only partial-span suction on the leading-edge flap.

NOTATION

a fuselage station measured from the nose, ft

b wing span, ft

c chord, measured parallel to the plane of symmetry, ft

$\bar{c}$ mean aerodynamic chord, $\frac{2}{S}\int_0^{b/2} c^2 dy$, ft

C_D drag coefficient, $\frac{\text{drag}}{q_o S}$

c_l section lift coefficient, $\frac{1}{c}\oint P\, dx \cos\alpha - \frac{1}{c}\oint P\, dz \sin\alpha$

C_L lift coefficient, $\frac{\text{lift}}{q_o S}$

C_m pitching-moment coefficient referred to quarter-chord point of mean aerodynamic chord, $\frac{\text{pitching moment}}{q_o S \bar{c}}$

C_Q flow coefficient, $\frac{Q}{U_o S}$

p_o free-stream static pressure, lb/sq ft

p_l local static pressure, lb/sq ft

P	airfoil pressure coefficient, $\frac{p_l-p_o}{q_o}$
P_d	average duct pressure coefficient, $\frac{p_d-p_o}{q_o}$
P_p	plenum-chamber pressure coefficient, $\frac{p_p-p_o}{q_o}$
q_o	free-stream dynamic pressure, lb/sq ft
Q	volume of air removed through porous surface, cu ft/sec, based on standard density at sea level
S	wing area, sq ft
t	thickness of porous material, in.
U_o	free-stream velocity, fps
w	suction air velocity, fps
$\frac{W}{S}$	assumed wing loading of airplane, lb/sq ft
x	chordwise distance parallel to plane of symmetry, ft
y	spanwise distance perpendicular to plane of symmetry, ft
z	distance perpendicular to chord of airfoil, ft
α	angle of attack referred to fuselage center line, deg
δ	flap deflection, deg
Δp	pressure drop across porous material, lb/sq ft

Subscripts

F	trailing-edge flap
N	leading-edge flap
crit	critical

MODEL AND APPARATUS

A general view and the geometric characteristics of the model are shown in figures 1 and 2, respectively. Except for the leading-edge and

trailing-edge flaps, the model was the same as that tested in references 1 and 2. The wing panels were from an F-86A airplane, having 35° of sweep at the quarter-chord line, an aspect ratio of 4.785, and a taper ratio of 0.513. The wing root and tip airfoil sections perpendicular to the quarter-chord line were modified NACA 0012-64 and 0011-64, respectively. The coordinates for these sections are given in reference 2. Flush orifices were located on the upper and lower surfaces of the wing and flaps at 0.25-, 0.45-, 0.65-, and 0.85-semispan stations to obtain the chordwise pressure distributions. Chordwise locations of the pressure orifices are given in table I.

The horizontal tail was also from an F-86A airplane and was mounted in the same position relative to the wing as it was on the airplane. The fuselage was of circular cross section and housed the pumping equipment used for area suction.

Leading-Edge Flap

The original wing structure ahead of the front spar was replaced with a new structure to allow the deflection of a leading-edge flap with ducting. The forward portion of the wing was hinged on the lower surface along the 11-percent-chord line measured perpendicular to the quarter-chord line. Thus, the forward portion of the wing could be deflected to the desired angle and held in place by an insert. Three inserts were employed in the present test. These inserts enabled testing of the plain wing (undeflected flap), a 30° deflection with no porous area, and a 40° deflection with and without porous area. Details of the 40° leading-edge flap and the ducts are shown in figure 3.

For the purpose of locating the position of the porous opening on the 40° flap, a reference line was located on the upper surface of the wing at the midpoint of the circular arc. The beginning of this circular arc was tangent to the upper surface of the wing and, consequently, began 8° forward of the projection of the hinge line (fig. 3). The reference line is approximately the 7-percent-chord line in the plan view with the flap deflected. This reference line was chosen because the location of the peak negative pressure was expected to be near it, and, hence, the openings could be conveniently measured. The forward and rearward edges of the metal mesh surface were, respectively, 2 percent of the chord ahead and 5 percent behind the reference line. The porous material on the 40° nose flap consisted of metal mesh backed by hard wool felt. The metal mesh was 0.008-inch thick with a ratio of open area to total area of 0.11 and with 4225 holes per square inch. The felt backing was tapered to provide the desired pressure-drop characteristics and so reduce the total quantity of air flow, as explained in reference 2. Figure 4 shows the thickness variation of the felt which was based on preliminary pressure distributions obtained with the nose flap

deflected 40° and with no porous area. Figure 5 shows the suction air velocity for a given pressure drop for a 1/2-inch thickness of the felt. For a given velocity of flow, the required pressure drop varied directly with the thickness. The position and extent of porous surface were varied both chordwise and spanwise by covering part or all of the surface with nonporous plastic tape. The various full-span configurations tested are listed in table II.

In addition to the full-span nose flap, tests were made of a partial-span nose flap. This configuration consisted of a 40° deflection of the flap from the wing tip inboard to 0.53 semispan, and 0° deflection from this point into the fuselage. This flap was tested with the porous area completely sealed and also with porous area configuration 1 (table II) on the deflected part.

Trailing-Edge Flap

The 55° trailing-edge area-suction flap had a constant chord, extended from 0.14 to 0.50 semispan, and had a porous area at the knee. The same flap was tested in reference 1. The porous area consisted of the same metal mesh as that used on the nose flap, backed by 1/16-inch soft wool felt. The flow characteristics of a 1/2-inch-thick sample of this felt are shown in figure 5. The reference line on the trailing-edge flap was the projection of the flap hinge line on the upper surface (fig. 3). An undeflected flap was simulated by removing the flap and completing the wing contour with a metal insert. Detail photographs of the leading-edge and trailing-edge flaps are given in figure 6.

Suction Apparatus

The suction systems for the leading-edge and trailing-edge flaps were similar but independent of each other. The air was drawn through the porous surfaces into the ducts and thence to the two separate plenum chambers in the fuselage. Centrifugal compressors driven by variable-speed electric motors located in the plenum chambers exhausted the air to the free stream through ducts located under the fuselage. The air-flow rates were determined at each exit from measurements made with total- and static-pressure tubes and thermocouples. Plenum-chamber and duct pressures were measured with static-pressure orifices and could be assumed to be equal to total pressures since the velocities of the air in the ducts and plenum chambers were low. The power required by each of the compressors was determined from the measurement of the power input and efficiency for each of the electric motors.

TESTS AND PROCEDURE

Tests

Three-component force data were obtained for all configurations listed in table III for a large angle-of-attack range for free-stream velocities varying from 112 to 166 feet per second (corresponding Reynolds numbers of 5.8×10^6 to 8.7×10^6).

External-surface pressure distributions over the wing and flap were observed and recorded for all configurations tested.

The suction requirements – flow coefficient, plenum-chamber pressure coefficient, and measured suction power (power input to the compressor) – were measured for the leading-edge and trailing-edge area-suction flaps. To obtain these suction requirements for a fighter airplane similar to the F-86A without interpolation and accompanying assumptions, data were measured at free-stream velocities varying with angle of attack. These velocities corresponded to those encountered by an airplane having wing loadings of 40 and 60 pounds per square foot. The pressures in the ducts were also measured, and the average values of the pressure coefficients for the nose flap are given in table IV. The difference between the duct and plenum-chamber pressure coefficients for the trailing-edge flap was small, and, therefore, the values of duct-pressure coefficient are not given. The velocities in the ducts and plenum chambers were low; therefore, the static pressures in the ducts and plenum chambers can be assumed to be equal to the total pressures. These pressures were used to obtain the pump and duct losses given in table IV.

Test Procedure

In the initial tests of the leading-edge area-suction flap, it was found that as suction was increased, the lift coefficient first increased rapidly and then very slowly. The accompanying sketch shows a typical variation of lift coefficient with flow coefficient. Observations of the chordwise pressure distributions indicated that the air-flow separation from the forward portion of the wing was eliminated when the lift coefficient ceased increasing rapidly. The flow coefficient corresponding to this condition will henceforth be referred to as the critical flow coefficient, $C_{Q_{crit}}$. In this investigation,

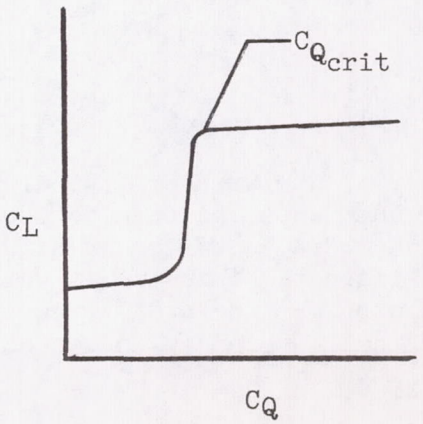

attention will be directed toward $C_{Q_{crit}}$ and the corresponding lift coefficient because the additional small increases in lift coefficient that could be obtained above $C_{Q_{crit}}$ were not considered to be of practical importance. Similar observations were made for the NACA trailing-edge area-suction flap used in this investigation and in reference 1.

The test procedure followed was to vary the flow coefficient for the leading-edge area-suction flap while the flow coefficient for the trailing-edge area-suction flap was maintained above $C_{Q_{crit}}$. For each value of flow coefficient, the lift, drag, pitching moment, and the duct and plenum-chamber pressures were measured. Suction requirements for the trailing-edge area-suction flap were obtained in a similar manner. This procedure was followed for each configuration tested for each angle of attack and free-stream velocity for which the data were desired. The value of $C_{Q_{crit}}$ was then determined from analysis of the force and pressure data.

It was found that below 25° angle of attack the variation of lift coefficient with flow coefficient for the nose flap could be obtained either by decreasing the flow coefficient from above $C_{Q_{crit}}$ or by increasing the flow coefficient from zero. However, at higher angles of attack, it was not possible to reattach the flow over the wing without reducing the angle of attack to about 24°. Therefore, to obtain suction requirements at these high angles of attack it was necessary to begin with unseparated flow and then to reduce the flow coefficient. In contrast, the variation of lift coefficient with flow coefficient for the trailing-edge flap could be obtained throughout the angle-of-attack range by decreasing the flow coefficient from above $C_{Q_{crit}}$ or by increasing the flow coefficient from zero.

The three-component force data up to the maximum lift coefficient, $C_{L_{max}}$, presented in this report are for the flow conditions existing on the wing when the flow coefficients for the leading-edge and/or trailing-edge area-suction flaps were at or slightly above $C_{Q_{crit}}$. Beyond $C_{L_{max}}$ the force data are presented at $C_{Q_{crit}}$ for $C_{L_{max}}$.

CORRECTIONS

The standard tunnel-wall corrections for a straight wing of the same area and span as the sweptback wing were applied to angle-of-attack and drag coefficient data. This procedure was followed since an analysis indicated that tunnel-wall corrections were approximately the same for straight and swept wings of the size under consideration. The increments that were added to the data are as follows:

$$\Delta\alpha = 0.61\ C_L$$

$$\Delta C_D = 0.0107\ C_L^2$$

$$\Delta C_m = 0.008\ C_L$$

No corrections were made for the drag of the exposed portion of the strut and its interference with the wing. Limited available data indicate this drag to vary from a drag coefficient of about 0.004 at 0 lift coefficient to 0 at 30° angle of attack.

All values of flow coefficient and measured suction horsepower were corrected for leakage resulting from construction and junctures. All flow coefficients were corrected to standard sea-level conditions. The effect of the thrust of the exhausting jets on the aerodynamic characteristics was negligible.

RESULTS AND DISCUSSION

Full-Span Leading-Edge Flap With 55° Trailing-Edge Area-Suction Flap

Force characteristics.- The aerodynamic characteristics for the 35° swept-wing model with different full-span leading-edge flaps are presented in figure 7. Included for comparative purposes are data for the same model, but with full-span leading-edge area suction (area suction applied to the leading edge of the plain wing, ref. 1). The data shown in figure 7 are for the model with a 55° trailing-edge area-suction flap. It was found that on this 35° swept wing, the spanwise progression of air-flow separation was so rapid that, for practical purposes, the maximum lift coefficient, $C_{L_{max}}$, is indicative of the initial occurrence of air-flow separation from the forward portion of the wing. Therefore, to indicate the delay in air-flow separation that was obtained with the different leading-edge configurations, the $C_{L_{max}}$'s are summarized below:

δ_N	Leading-edge configuration	$C_{L_{max}}$	α for $C_{L_{max}}$
0°	Undeflected leading-edge flap (plain wing)	1.60	13.0
30°	Plain leading-edge flap	1.78	16.1
40°	Plain leading-edge flap	1.78	16.1
0°	Leading-edge area suction (plain wing, ref. 1)	2.23	25.4
40°	Leading-edge area-suction flap	2.44	29.5

These data indicate that air-flow separation from the leading edge of the wing was delayed to a higher angle of attack by the application of area suction to the knee of the 40° nose flap than by the application of leading-edge area suction. In addition, the peak surface pressure coefficients over the knee of the leading-edge flap were much less negative than those at the leading edge of the undeflected nose flap at the same angle of attack (fig. 7(b)).

The force characteristics for the model with the leading-edge area-suction flap presented in figure 7 are representative for all the free-stream velocities that were tested. In addition, they are representative for all porous openings of 1-1/2 inches or greater, provided that the flow coefficients were equal to or greater than $C_{Q_{crit}}$ for the respective openings. For these porous-area configurations, the maximum lift coefficient, $C_{L_{max}}$, was limited by separation of the air flow from the leading edge of the deflected nose flap. Therefore, it would be expected that separation could be delayed to a higher angle of attack, if desired, by increasing the deflection of the nose flap. It was felt that increasing $C_{L_{max}}$ by increasing the nose-flap deflection on this 35° swept-wing model would be of no practical importance because of the high angles of attack encountered. However, on wings with greater sweep angles or with thinner airfoil sections, it may be necessary to use a larger deflection on the leading-edge area-suction flap to obtain the desired delay in air-flow separation.

Observation of the pressure distribution indicated that the loss in lift and slight increase in drag at angles of attack below 0° resulted from air-flow separation from the lower surface of the deflected leading-edge flap. Deflecting the leading-edge flap also resulted in a shift in the pitching-moment curve because of the rearward movement in the center of pressure (fig. 7(b)).

Suction requirements.- The suction requirements for the full-span leading-edge area-suction flap deflected 40° with porous-area configuration 1 (table II) are given in figure 8 for free-stream velocities corresponding to wing loadings of 40 and 60 pounds per square foot. (It will be shown later that the lowest flow requirements for the full-span, leading-edge, area-suction flap of this investigation were obtained with this porous-area configuration.) Corresponding values for full-span leading-edge area suction (ref. 1) are also presented in this figure. The comparison of suction requirements is summarized on the following page:

W/S = 40 pounds per square foot										
α	C_L	U_o, ft/sec	Leading-edge area-suction flap, $\delta_N = 40^\circ$				Leading-edge area suction (plain wing, ref. 1)			
			$C_{Q_{crit}}$	P_p	Measured suction, hp	Suction, hp[1]	$C_{Q_{crit}}$	P_p	Measured suction, hp	Suction, hp
17.2	1.83	136	0.00022	-6.2	3.7	1.9	0.00051	-19.4	36.4	23.7
21.3	2.07	128	.00040	-7.5	7.0	3.9	.00081	-30.0	63.3	36.0
23.4	2.17	125	- - -	- - -	- -	- -	.00101	-38.0	97.6	45.4
25.4	2.27	122	.00062	-10.1	11.5	6.8	- - -	- - -	- - -	- - -
29.5	2.44	117	.00122	-15.3	38.8	19.3	- - -	- - -	- - -	- - -
W/S = 60 pounds per square foot										
17.2	1.83	166	.00026	-6.0	6.7	4.1	.00061	-19.8	77.9	43.1
21.3	2.07	156	.00035	-7.4	10.5	6.2	.00088	-31.4	171.0	92.0
25.4	2.27	149	.00061	-9.7	23.4	12.4	- - -	- - -	- - -	- - -
29.5	2.44	144	.00118	-14.5	67.0	32.7	- - -	- - -	- - -	- - -

[1]Suction horsepower is equal to the measured suction horsepower minus the pump loss and duct loss which are listed in table IV for the leading-edge area-suction flap (40°).

For a given angle of attack, the power required to maintain unseparated flow on the wing with the leading-edge area-suction flap was only about one-tenth of that required for leading-edge area suction. This reduction in power was caused by the less negative pumping-pressure coefficient and lower flow coefficient which resulted from the much lower negative surface pressure coefficient and less adverse pressure gradient at the knee of the nose flap (fig. 7(b)). It should be noted that the $C_{L_{max}}$ for the leading-edge area-suction flap (40°) was higher than the $C_{L_{max}}$ for leading-edge area suction. If the $C_{L_{max}}$ for these two methods of boundary-layer control had been the same, a more equitable comparison of suction requirements would have been obtained. Equal $C_{L_{max}}$'s could have been obtained by reducing the deflection of the leading-edge flap to reduce the $C_{L_{max}}$ or by increasing the chordwise extent of the porous opening for leading-edge area suction to increase $C_{L_{max}}$ (ref. 2). If either of these two changes had been made, the advantage of using a leading-edge area-suction flap from the standpoint of suction requirements would have been even greater than that shown in the preceding table and in figure 8. The suction requirements for the 55° trailing-edge area-suction flap, when used in conjunction with the nose flap, are given in table V.

The variation of lift coefficient with flow coefficient for the leading-edge area-suction flap deflected 40° is shown in figure 9 for

several angles of attack. These variations are shown for porous-area configuration 1 (table II) at free-stream velocities corresponding to a wing loading of 40 pounds per square foot. The reflexes in the curves near $C_{Q_{crit}}$ (fig. 9) occurred because the pump was operating at a condition from which a large decrease in pressure ratio (caused by collapse of external peak pressures) at approximately constant speed resulted in an increased flow quantity. It was noted previously in Test Procedure that above 24° angle of attack, the flow could not be reattached by increasing the flow coefficient; this hysteresis is also shown in figure 9. An airplane utilizing a leading-edge area-suction flap could maintain unseparated air flow by maintaining the flow coefficient above $C_{Q_{crit}}$ as the angle of attack was increased; therefore, the $C_{L_{max}}$ of this flap could be attained. However, if the angle of attack is increased beyond the angle for $C_{L_{max}}$, the airplane would stall abruptly. To permit recovery from this stall, the angle of attack would have to be reduced to 24° or less; at this lower angle of attack, the air flow could reattach because of the excess flow coefficient available due to the lower $C_{Q_{crit}}$ at this angle. Generally, the stall recovery of an operational airplane entails a reduction in angle of attack; therefore, the hysteresis encountered with the nose flap would probably not result in any unusual operational problems. However, at the present time, it is not possible to determine the acceptability of the stall characteristics of an airplane from wind-tunnel tests alone.

The shapes of the curves presented in figure 9 and the $C_{Q_{crit}}$ were affected by the position and chordwise extent of the porous opening. However, the lift coefficient at $C_{Q_{crit}}$ was unchanged at angles of attack below $C_{L_{max}}$. The $C_{L_{max}}$ was the same for all chordwise extents of 1-1/2 inches and greater; for a chordwise extent of 3/4-inch (configuration 9), the $C_{L_{max}}$ was reduced to 2.35. The variation of the $C_{Q_{crit}}$ with position and chordwise extent of porous opening is shown in figure 10 for several angles of attack and for a free-stream velocity of 145 feet per second. For the porous configurations tested, the lowest flow coefficients and plenum-chamber pressure coefficients were obtained with the forward edge of the opening at the reference line and a 2-1/2-inch opening along the full span (porous-area configuration 1). Decreasing the opening at the root while maintaining the 2-1/2-inch opening at the tip (configurations 10, 11, and 12, table II) did not result in a further reduction of the flow coefficients. It should be noted that above 16° angle of attack, the peak external pressures were 1/2 to 1 inch forward of the reference line. Since only one felt design was tested, and since this one had a constant thickness forward of the reference line, the $C_{Q_{crit}}$ might be reduced by further tests with additional felt designs. In addition, these tests might indicate an optimum opening with the forward edge closer to the location of the peak external pressures. In the present investigation, it was found that the $C_{Q_{crit}}$ for a given configuration and angle of attack did not vary with free-stream velocity in the range tested (112 to 166 fps). In addition,

the required plenum-chamber pressure coefficient for a given angle of attack did not vary in this range of free-stream velocities. Consequently, for a given angle of attack, the suction power required for the leading-edge area-suction flap was proportional to the cube of the free-stream velocity for the velocity range investigated (112 to 166 fps).

Pressure distributions.- The chordwise pressure distributions for the model having a 40° leading-edge flap and a 55° trailing-edge area-suction flap are shown in figure 11 at four spanwise stations for several angles of attack. These distributions are typical for all chordwise extents of porous area of 1-1/2 inches or greater. Below 16° angle of attack, applying area suction at the knee of the nose flap did not affect the pressure distributions. By comparing the peak negative pressures for the 85-percent spanwise station at 25° and 29° angle of attack (figs. 11(e) and 11(f)), it can be seen that the air flow has started to separate from the leading edge of the wing at 29°. At 30° angle of attack, the peak pressures at the leading edge and knee have collapsed at all four pressure stations as the air-flow separation has spread over the entire wing.

The section-lift curves shown in figure 12 were obtained by the integration of the chordwise pressure distributions.

Effect of Trailing-Edge Area-Suction Flap on Characteristics of 40° Full-Span Leading-Edge Area-Suction Flap

Force characteristics.- Three-component force data for the 35° swept-wing model with the full-span leading-edge area-suction flap deflected 40° and an undeflected trailing-edge flap are presented in figure 13. Included for comparative purposes are data for the same suction nose flap with the 55° trailing-edge area-suction flap. It is seen that the angle of attack for $C_{L_{max}}$ was not affected by the trailing-edge flap, and that the 55° trailing-edge area-suction flap provided a large increment of lift throughout the angle-of-attack range. Comparison of the slope of the section-lift curves (fig. 12) at the trailing-edge-flap stations ($2y/b = 0.25$ and 0.45) with those for the unflapped stations ($2y/b = 0.65$ and 0.85) indicates a decrease in trailing-edge-flap effectiveness with increasing angle of attack. This decrease can also be noted in figure 13 by comparing the trailing-edge-flap lift increment at low angles of attack with that at high angles of attack. Since this trailing-edge-flap lift increment was equal to that reported in reference 1 for the unflapped leading edge, the effectiveness of the trailing-edge area-suction flap was not altered by deflecting the leading-edge flap. This substantiates the previously noted observation that the loss in lift and slight increase in drag at negative angles of attack were due to air-flow separation from the lower surface of the deflected leading-edge flap.

Suction requirements.- The suction requirements for the 40° leading-edge area-suction flap with an undeflected trailing-edge flap are given in figure 14. Included for comparative purposes are the suction requirements for the same leading-edge flap with the 55° trailing-edge area-suction flap. These suction requirements are presented for a wing loading of 40 pounds per square foot. A comparison at equal lift coefficients shows that the suction requirements for the nose flap of the model with an undeflected trailing-edge flap were greater than those for the model with the 55° trailing-edge area-suction flap. These larger suction requirements resulted from the more negative surface pressure coefficients caused by the added angle of attack required to produce an amount of lift equal to the trailing-edge-flap lift increment. A comparison at equal angles of attack indicates that the suction requirements for the nose flap of the model with an undeflected trailing-edge flap were less than those for the model with the deflected trailing-edge flap. This reduction in suction requirements resulted primarily from the less negative surface pressure coefficients over the entire upper surface of the wing when the deflection of the trailing-edge flap was reduced.

Full-Span 40° Leading-Edge Flap With Partial-Span Suction and Partial-Span 40° Leading-Edge Area-Suction Flap, Both With 55° Trailing-Edge Area-Suction Flap

Although the necessity of having a pitch-down moment at $C_{L_{max}}$ to have acceptable stall characteristics is open to question (ref. 8), a limited study was made to determine if a favorable change in pitching moment at $C_{L_{max}}$ could be obtained by applying partial-span area suction to the full-span or to a partial-span nose flap. The results of this limited study of the full-span and partial-span nose flap are presented in figures 15 and 16, respectively. Although changes in the pitching moment were produced, none of the modifications resulted in a pitch-down moment at $C_{L_{max}}$.

As was noted in references 1 and 2 for leading-edge area suction, a lower $C_{L_{max}}$ was incurred by using partial-span suction on the nose flap rather than full-span suction. In the present test it was found that the $C_{Q_{crit}}$ for partial-span suction at a lift coefficient of 1.83 was about the same as for full-span suction. At lift coefficients of 2.07 and 2.23, $C_{Q_{crit}}$ for partial-span suction was about 0.0001 less than for full-span suction. Large changes in flow coefficient above $C_{Q_{crit}}$ did not change the pitching-moment coefficient.

CONCLUDING REMARKS

In this investigation of a 35° swept-wing model the aerodynamic characteristics and suction requirements of a leading-edge area-suction flap deflected 40° were determined. These characteristics and requirements were compared with those obtained for leading-edge area suction (area suction applied to the leading edge of a plain wing) in a previous investigation on the same model. This comparison showed that a comparable delay in air-flow separation from the forward portion of the wing was obtained with the leading-edge area-suction flap and that the power required to obtain a given lift coefficient was only one-tenth of that required for leading-edge area suction. This large reduction in power resulted from the lower flow coefficients and less negative plenum-chamber pressure coefficients, each being about one-third of those required for leading-edge area suction.

The 40° leading-edge area-suction flap delayed the air-flow separation from an angle of attack of 13° to 25° (from a lift coefficient of 1.60 to 2.27 when used with a 55° trailing-edge area-suction flap) with a flow coefficient of 0.0006 and 23 horsepower (including duct and pump losses) at a free-stream velocity of 149 feet per second. Approximately doubling the flow coefficient and suction pressure coefficient delayed the air-flow separation to 29° angle of attack. It was found that at a given angle of attack the flow coefficient and plenum-chamber pressure coefficients were not affected by free-stream velocity within the range of velocities tested (112 to 166 fps). Consequently, the suction power required at a given angle of attack varied with the cube of the free-stream velocity.

Deflecting the leading-edge flap did not alter the effectiveness of the trailing-edge area-suction flap. However, the suction requirements of the leading-edge flap for a given lift coefficient were reduced by deflecting the trailing-edge flap.

No large improvements in the pitching-moment coefficient at $C_{L_{max}}$ were obtained by applying partial-span area suction to the leading-edge flap. However, a large reduction in $C_{L_{max}}$ was incurred by applying partial-span suction.

Ames Aeronautical Laboratory
National Advisory Committee for Aeronautics
Moffett Field, Calif., Oct. 26, 1953

REFERENCES

1. Cook, Woodrow L., Holzhauser, Curt A., and Kelly, Mark W.: The Use of Area Suction for the Purpose of Improving Trailing-Edge Flap Effectiveness on a 35° Sweptback Wing. NACA RM A53E06, 1953.

2. Holzhauser, Curt A., and Martin, Robert K.: The Use of Leading-Edge Area Suction to Increase the Maximum Lift Coefficient of a 35° Swept-Back Wing. NACA RM A52G17, 1952.

3. Pasamanick, Jerome, and Scallion, William I.: The Effects of Suction Through Porous Leading-Edge Surfaces on the Aerodynamic Characteristics of a 47.5° Sweptback Wing-Fuselage Combination at a Reynolds Number of 4.4×10^6. NACA RM L51K15, 1952.

4. Cook, Woodrow L., and Kelly, Mark W.: The Use of Area Suction for the Purpose of Delaying Separation of Air Flow at the Leading Edge of a 63° Swept-Back Wing – Effects of Controlling the Chordwise Distribution of Suction-Air Velocities. NACA RM A51J24, 1952.

5. Dannenberg, Robert E., and Weiberg, James A.: Section Characteristics of a 10.5-Percent-Thick Airfoil With Area Suction as Affected by Chordwise Distribution of Permeability. NACA TN 2847, 1952.

6. Lemme, H. G.: Kraftmessungen und Druckverteilungsmessungen an einem Flugel mit Knicknase, Vorflügel, Wolbungs – und Spreiz-Klappe, Aerodynamische Versuchsanstalt Göttingen. E. V. Forshungsbericht Nr. 1676, October 15, 1942.

7. McCormack, Gerald M., and Cook, Woodrow L.: Effects of Several Leading-Edge Modifications on the Stalling Characteristics of a 45° Swept-Forward Wing. NACA RM A9D29, 1949.

8. Anderson, Seth B., Matteson, Frederick H., and Van Dyke, Rudolph D., Jr.: A Flight Investigation of the Effect of Leading-Edge Camber on the Aerodynamic Characteristics of a Swept-Wing Airplane. NACA RM A52L16a, 1953.

TABLE I.- LOCATION OF SURFACE PRESSURE ORIFICES FOR MODEL WITH 40° LEADING-EDGE FLAP AND 55° TRAILING-EDGE FLAP
[Position of orifices,[1] chordwise percent]

Orifice number	Upper surface			Lower surface	
	0.25, 2y/b	0.45, 2y/b	0.65 and 0.85, 2y/b	0.25 and 0.45, 2y/b	0.65 and 0.85, 2y/b
1	0	0	0	---	---
2	.19	.63	.19	1.2	1.2
3	.90	.90	.63	1.6	2.3
4	2.5	2.5	.90	2.3	3.6
5	4.3	3.4	3.4	3.0	11.7
6	6.1	4.3	4.3	3.6	20.0
7	6.3	6.1	6.1	4.1	40.0
8	7.1	6.5	6.5	6.8	60.0
9	7.9	8.1	7.2	9.3	80.0
10	8.7	9.0	8.1	11.7	97.5
11	9.6	10.0	9.1	15.0	---
12	10.6	10.9	9.9	20.0	---
13	11.5	11.9	11.1	30.0	---
14	12.5	12.9	12.1	40.0	---
15	15.0	20.0	13.2	60.0	---
16	20.0	30.0	20.0	70.0	---
17	30.0	40.0	30.0	75.0	---
18	40.0	50.0	40.0	80.0	---
19	50.0	70.0	60.0	88.0	---
20	60.0	75.0	70.0	93.2	---
21	70.0	80.0	80.0	98.0	---
22	75.0	82.1	90.0	---	---
23	80.0	83.0	97.5	---	---
24	84.0	84.0	---	---	---
25	84.4	84.4	---	---	---
26	84.8	87.0	---	---	---
27	85.4	91.0	---	---	---
28	85.7	95.0	---	---	---
29	87.0	99.0	---	---	---
30	91.0	---	---	---	---
31	95.0	---	---	---	---
32	99.0	---	---	---	---

[1]Orifices omitted:
0.65 2y/b upper 16
0.25 2y/b lower 5, 12, 15
0.45 2y/b lower 3

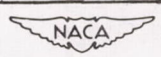

TABLE II.- POSITIONS AND CHORDWISE EXTENTS OF POROUS AREA TESTED

40° Leading-Edge Area-Suction Flap					
Porous-area configuration number	Position of forward edge,[a] in.	Extent of chordwise opening			
		Opening at 2y/b = 0.10		Opening at 2y/b = 0.96	
		Inches[b]	x/c[c]	Inches[b]	x/c[c]
1	0	2-1/2	0.025	2-1/2	0.045
2	1/2	2-1/2	.025	2-1/2	.046
3	1	2-1/2	.026	2-1/2	.047
4	-1/2	2-1/2	.024	2-1/2	.044
5	-1	2-1/2	.024	2-1/2	.042
6	-1/2	4	.040	4	.072
7	0	3-1/2	.035	3-1/2	.064
8	0	1-1/2	.015	1-1/2	.027
9	0	3/4	.007	3/4	.013
10	0	1-1/2	.015	2-1/2	.045
11	0	3/4	.007	2-1/2	.045
12	0	0	0	2-1/2	.045

55° Trailing-Edge Area-Suction Flap					
Porous-area configuration number	Position of forward edge,[a] in.	Extent of chordwise opening			
		Opening at 2y/b = 0.14		Opening at 2y/b = 0.50	
		Inches[b]	x/c[c]	Inches[b]	x/c[c]
4 (ref. 1)	2-1/2	2-1/2	0.016	2-1/2	0.020

[a]Measured normal to reference line along wing surface (positive is toward trailing edge)

[b]Measured from forward edge normal to reference line along wing surface, in.

[c]Ratio of local streamwise opening to local streamwise chord

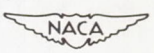

TABLE III.- MODEL CONFIGURATIONS TESTED AND TEST CONDITIONS

Figure number	Leading-edge flap					Trailing-edge flap		U_o, ft/sec	W/S, lb/sq ft
	δ_N, deg	Spanwise extent of flap		Spanwise extent of porous area		Chordwise porous-area configuration (table II)	δ_F, deg	Chordwise porous-area configuration (table II)		
		Inboard, 2y/b	Outboard, 2y/b	Inboard, 2y/b	Outboard, 2y/b					
7	0	---	---	---	---	none	55	4	145	varied
7	30	0.10	0.96	---	---	-do-	55	4	145	Do.
7	40	.10	.96	---	---	-do-	55	4	145	Do.
7,8	40	.10	.96	0.10	0.96	1	55	4	varied	40 and 60
7	40	.10	.96	.10	.96	1	55	4	112	varied
7	40	.10	.96	.10	.96	1-12	55	4	145	Do.
10	40	.10	.96	.10	.96	1-12 (6, 10-12 tested but not shown)	55	4	145	Do.
13,14	40	.10	.96	.10	.96	1	0	---	varied	40
15	40	.10	.96	.25	.96	1	55	4	112	varied
15	40	.10	.96	.45	.96	1	55	4	112	Do.
16	40	.53	.96	---	---	none	55	4	112	Do.
16	40	.53	.96	.53	.96	1	55	4	112	Do.

TABLE IV.- DUCT AND PUMP LOSSES FOR 40° LEADING-EDGE AREA-SUCTION FLAP USED WITH 55° TRAILING-EDGE AREA-SUCTION FLAP

W/S = 40 pounds per square foot					
C_L	U_o, ft/sec	P_{dN}	Duct loss, hp	Pump loss, hp	Measured suction, hp
1.83	136	-6.1	0	1.8	3.7
2.07	128	-7.4	0	3.1	7.0
2.27	122	-9.9	.3	4.4	11.5
2.44	117	-14.7	1.7	17.8	38.8
W/S = 60 pounds per square foot					
1.83	166	-5.9	0	2.6	6.7
2.07	156	-7.3	0	4.3	10.5
2.27	149	-9.5	.4	10.6	23.4
2.44	144	-13.8	3.5	30.8	67.0

TABLE V.- FLOW REQUIREMENTS FOR 55° TRAILING-EDGE AREA-SUCTION FLAP USED WITH 40° LEADING-EDGE AREA-SUCTION FLAP

W/S = 40 pounds per square foot				
C_L	U_o, ft/sec	C_{Q_F}	P_{p_F}	Measured suction, hp
2.07	128	0.00035	-3.0	3.5
2.27	122	.00040	-2.9	2.9
2.44	117	.00035	-2.7	2.2
W/S = 60 pounds per square foot				
2.07	156	0.00033	-2.8	4.6
2.27	149	.00037	-2.6	4.1
2.44	144	.00045	-3.0	4.9

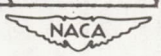

A-17969

Figure 1.- The 35° sweptback-wing model with the leading-edge and trailing-edge flaps deflected.

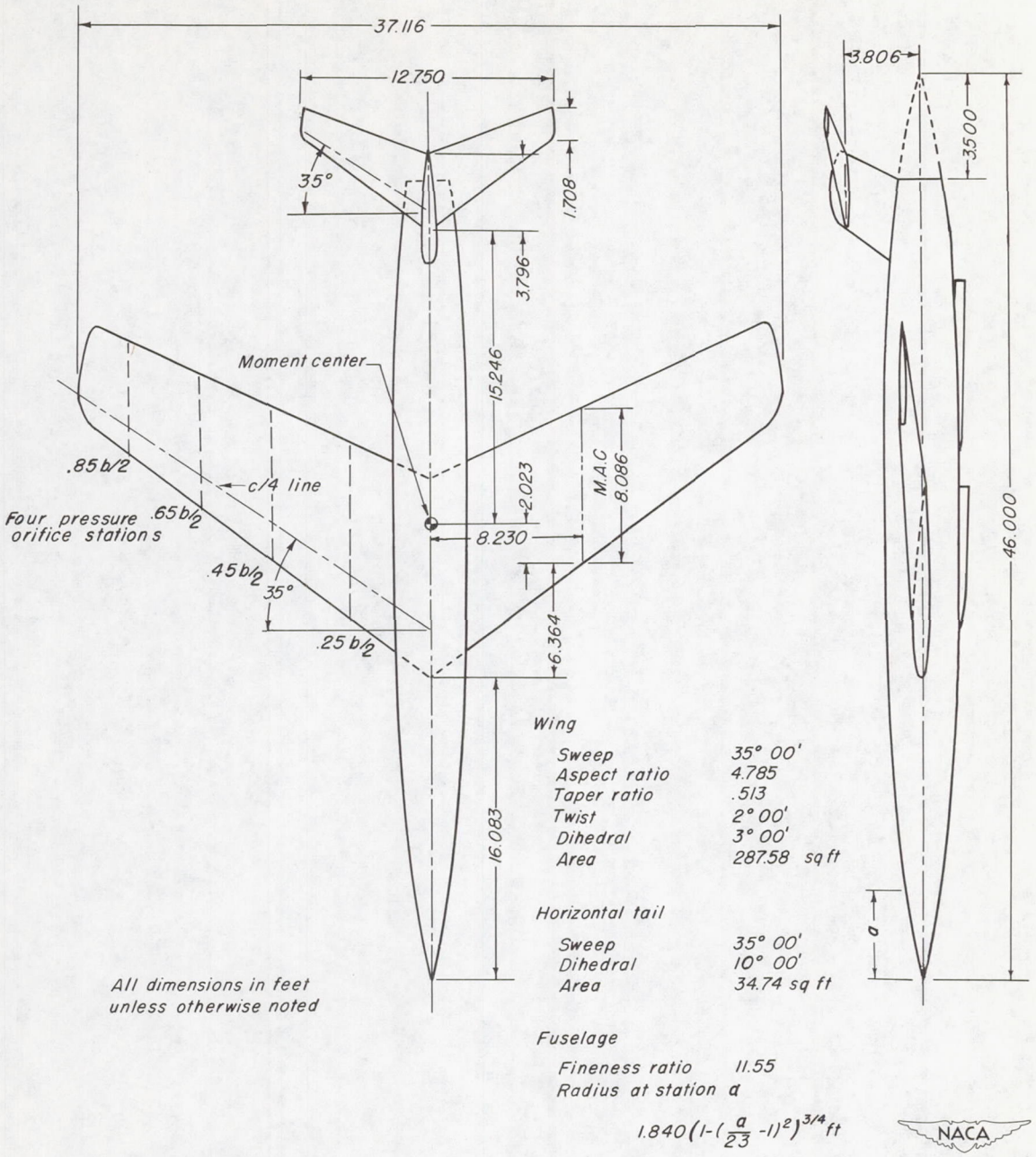

Figure 2.- Geometric characteristics of the 35° swept-wing model with undeflected flaps.

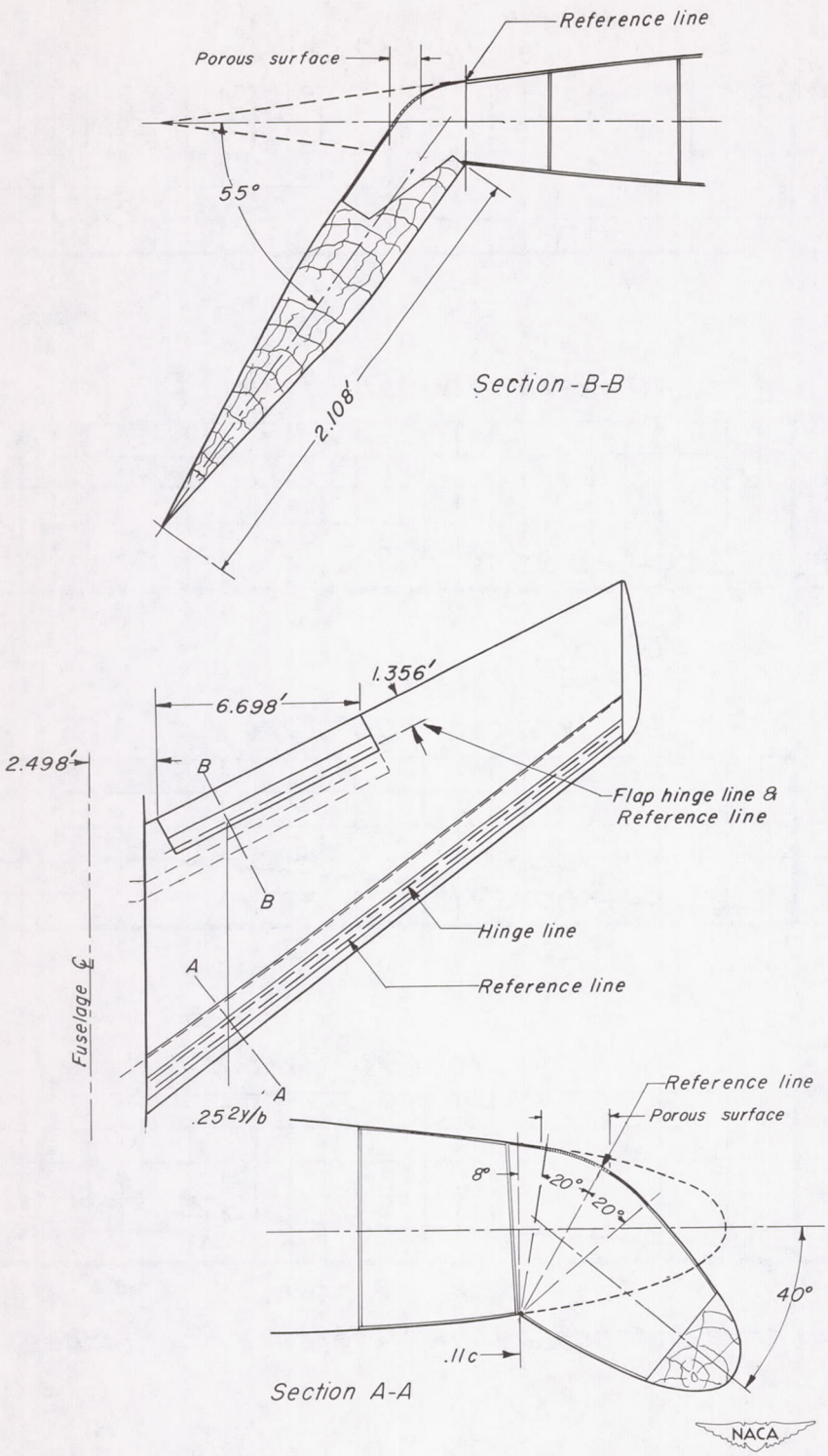

Figure 3.- Details of the flapped portions of the wing.

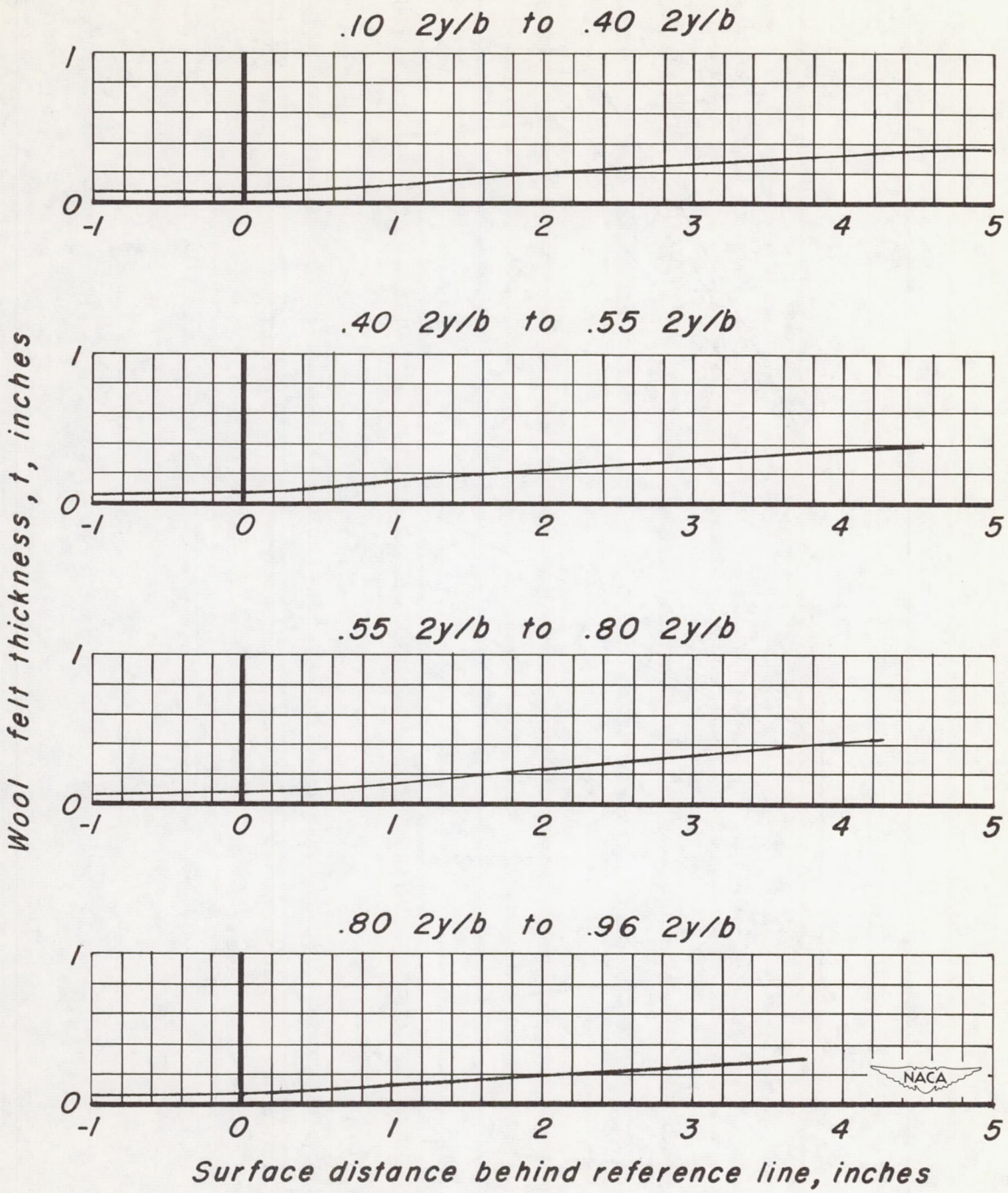

Figure 4.- Thickness variations of the felt backing used in the 40° leading-edge area-suction flap.

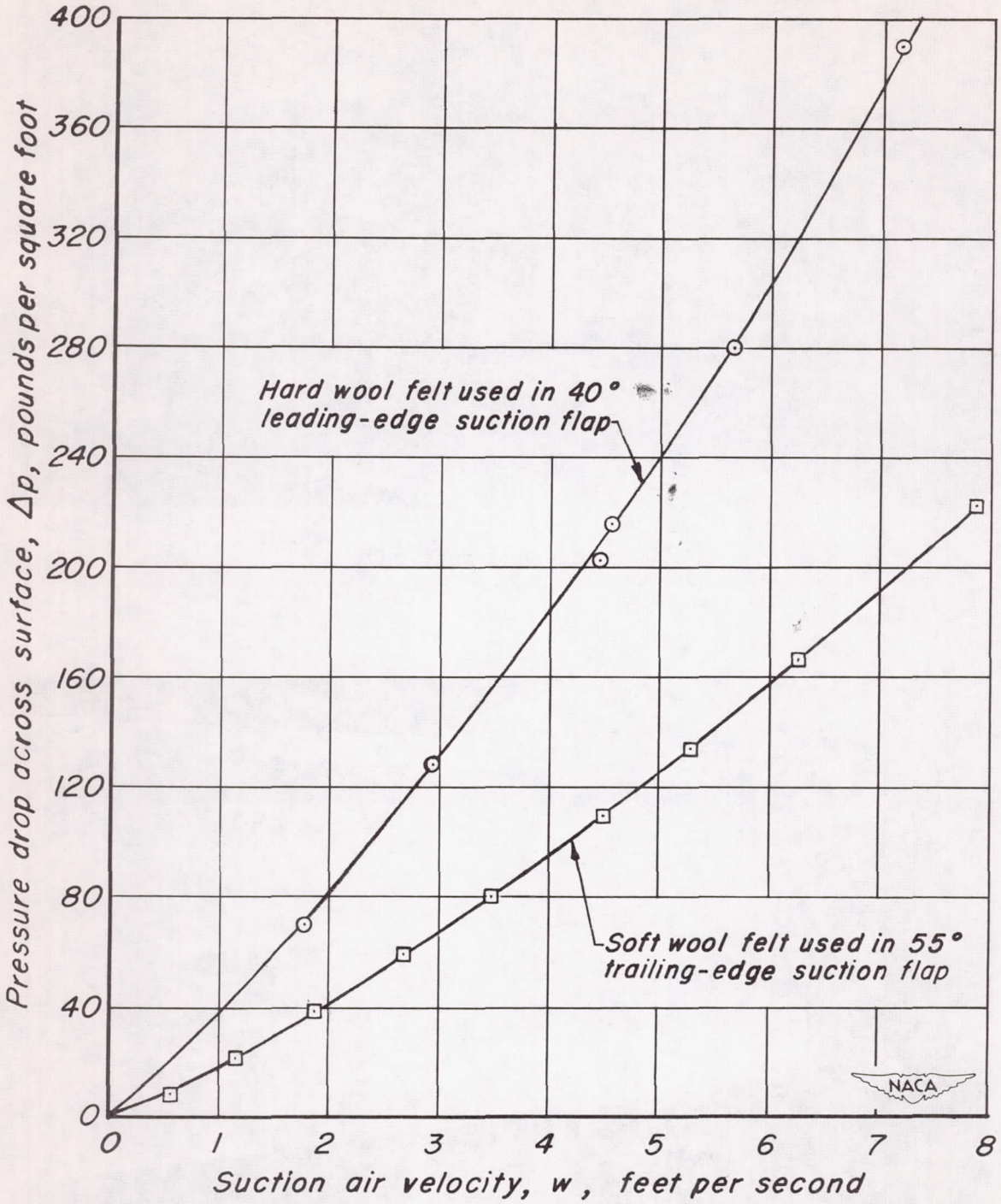

Figure 5.- Calibration of suction air velocities for the porous metal sheet backed with 1/2-inch wool felt material.

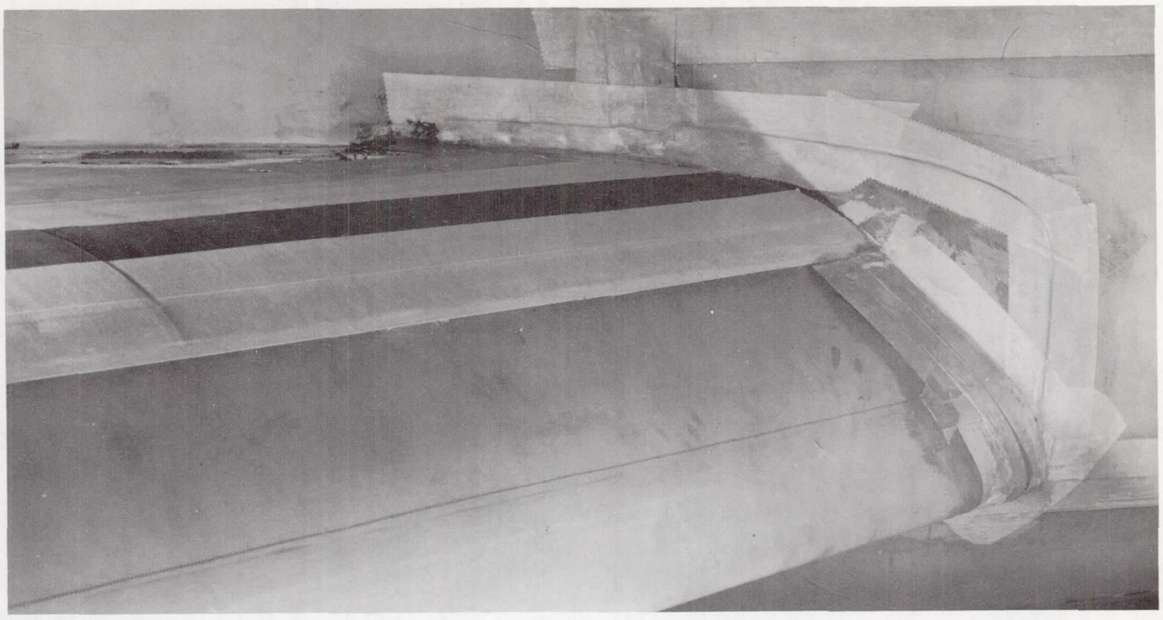

A-18044

(a) The 40° leading-edge area-suction flap.

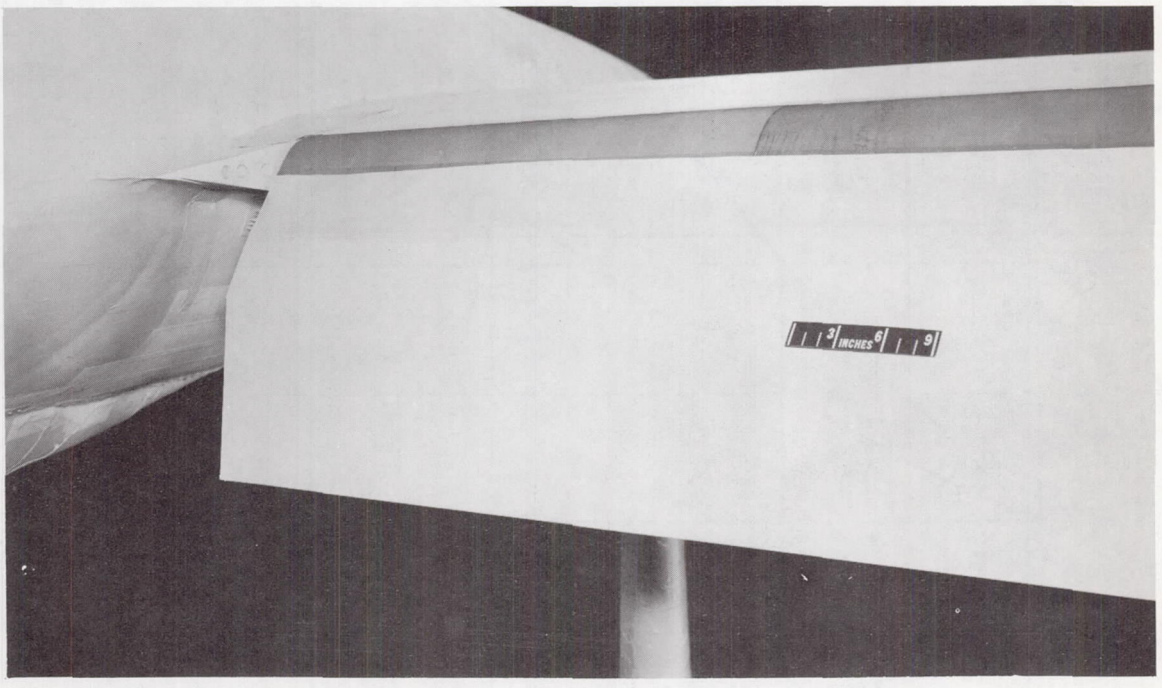

A- 17277

(b) The 55° trailing-edge area-suction flap.

Figure 6.- Close-up of the deflected flaps.

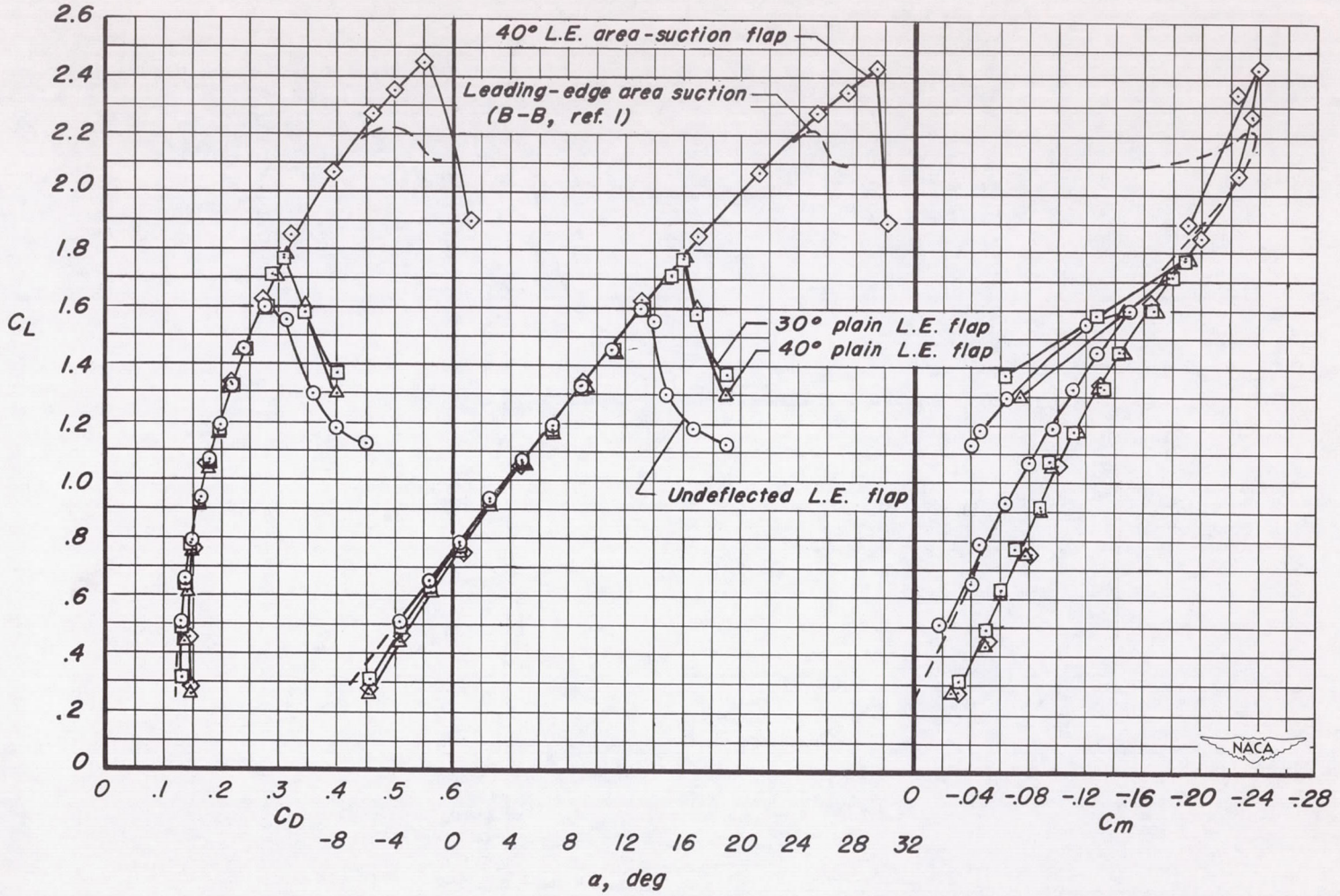

(a) C_D, C_L, C_m

Figure 7.- Comparison of the aerodynamic characteristics of the model having leading-edge flaps with those of model having leading-edge area suction; 55° trailing-edge area-suction flap.

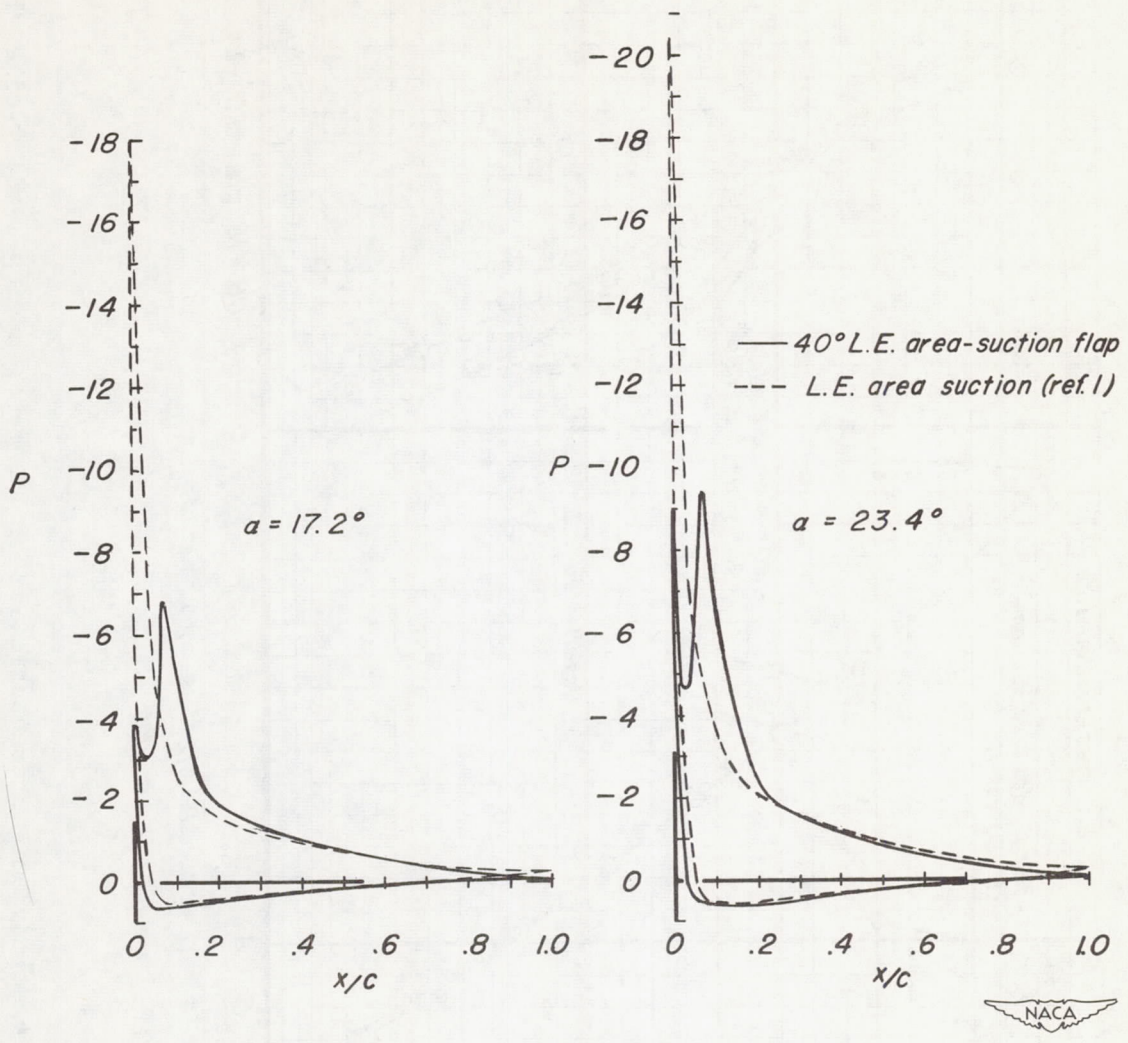

(b) Chordwise pressure distribution at 0.85-semispan station.

Figure 7.- Concluded.

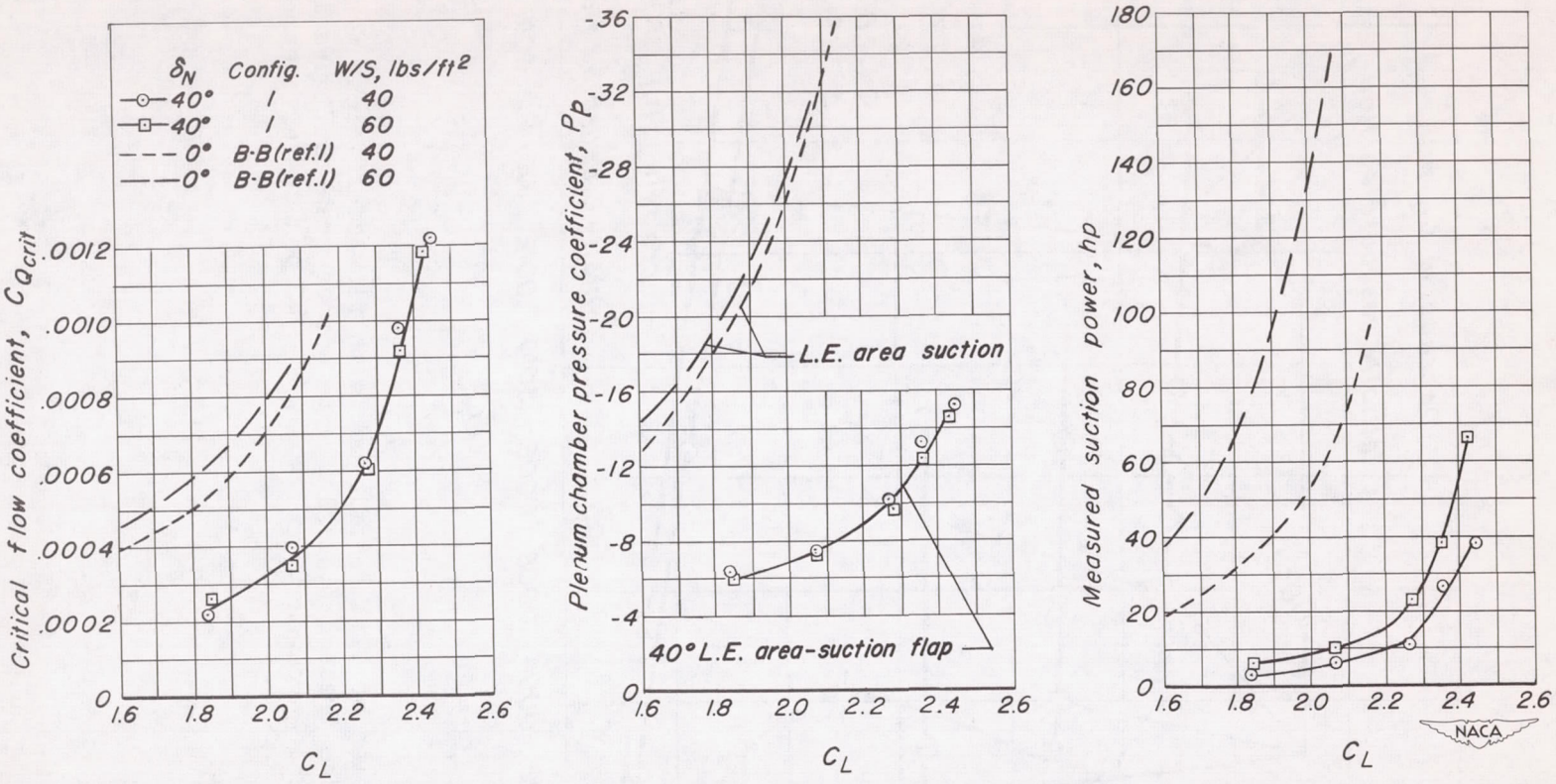

Figure 8.- Comparison of suction requirements for model having the full-span 40° leading-edge area-suction flap with those for model having full-span leading-edge area suction; 55° trailing-edge area-suction flap; W/S = 40 and 60 pounds per square foot.

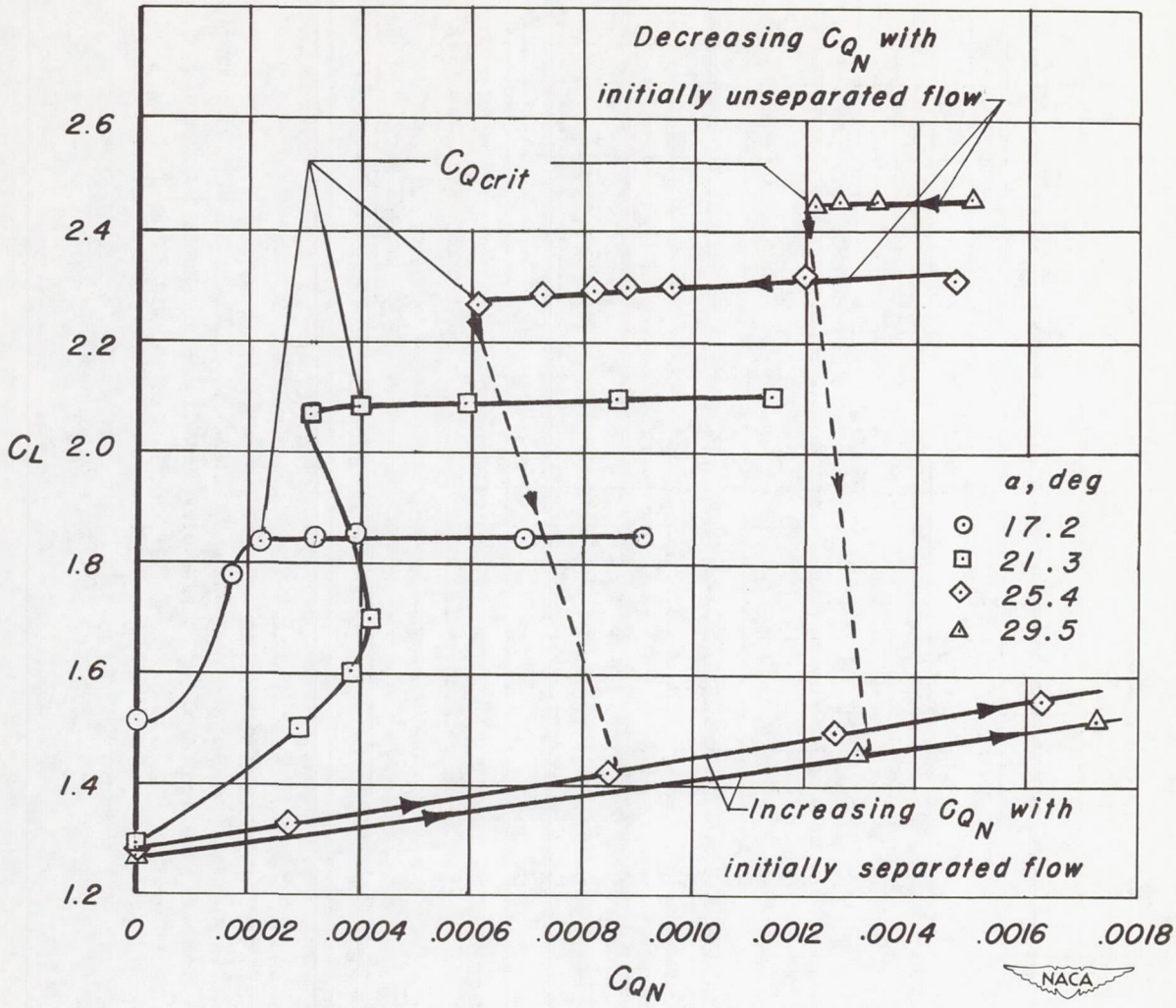

Figure 9.- Variation of lift coefficient with flow coefficient for the 40° leading-edge area-suction flap with porous-area configuration 1; 55° trailing-edge area-suction flap; W/S = 40 pounds per square foot.

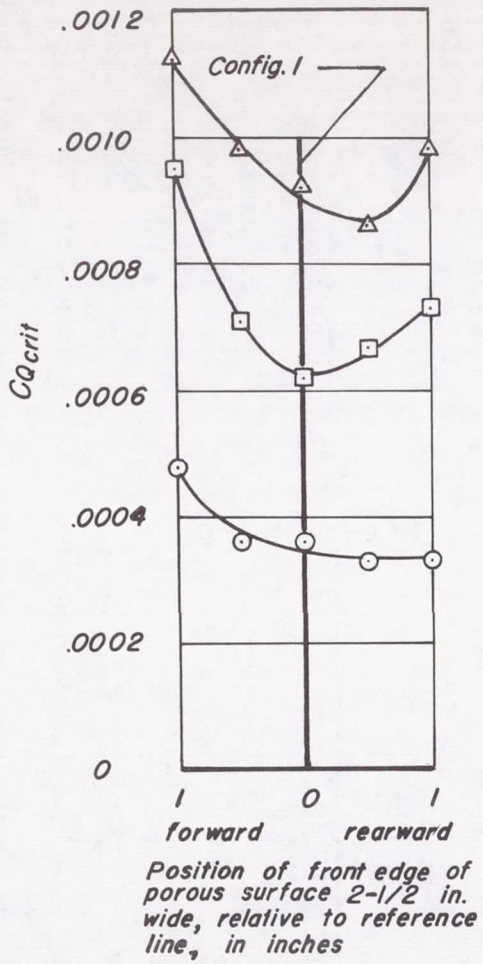

(a) Porous-surface position.

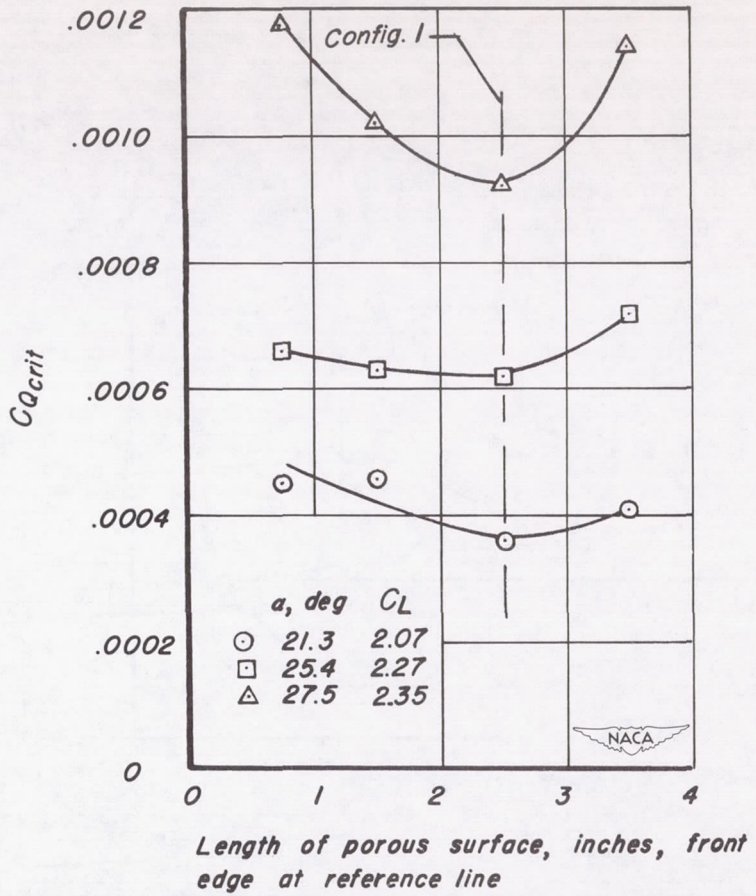

(b) Porous-surface extent.

Figure 10.- Variation of the critical flow coefficient with position and extent of porous surface on the 40° leading-edge area-suction flap; 55° trailing-edge area-suction flap; U_o = 145 feet per second.

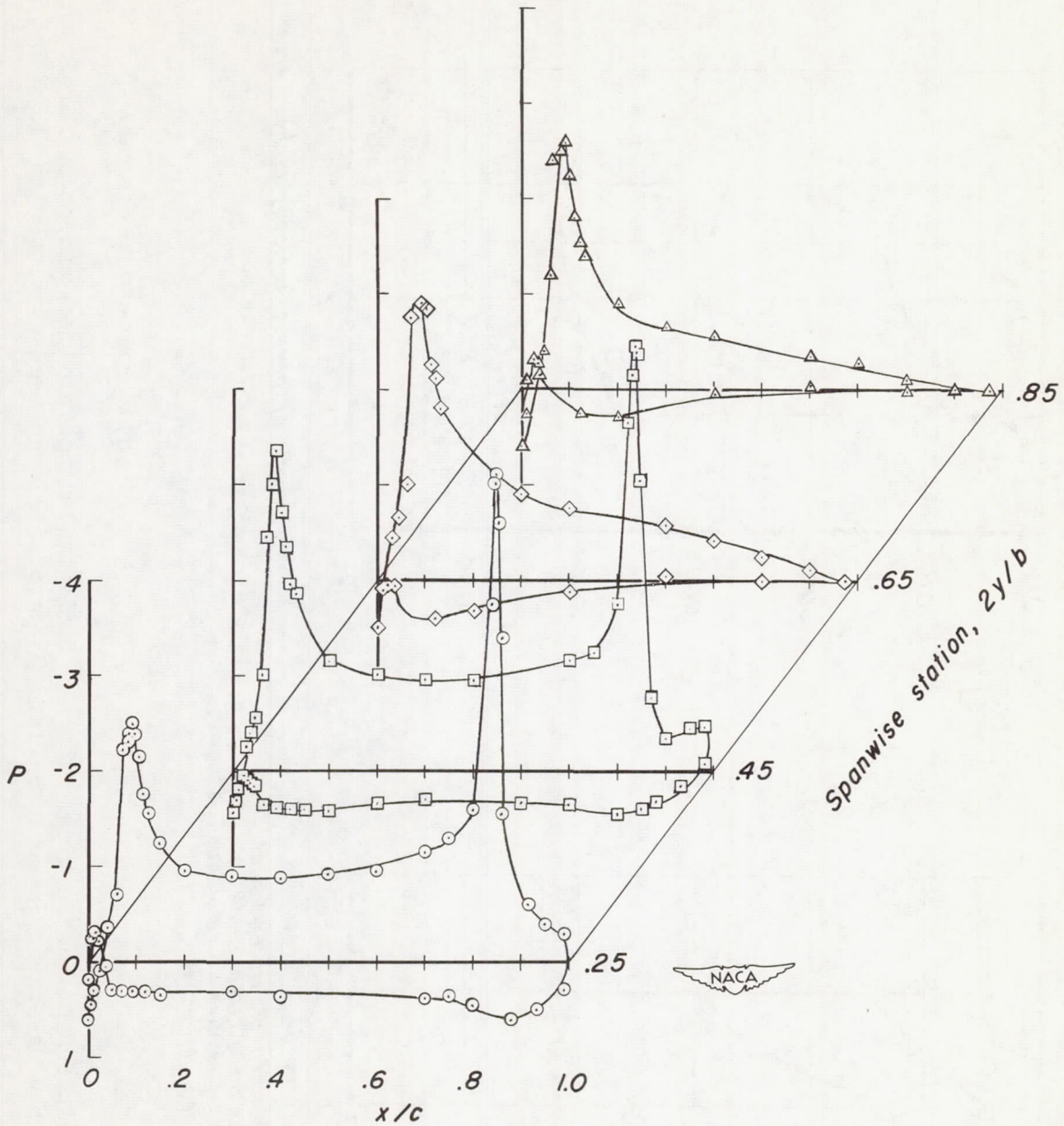

(a) $\alpha = 4.4^{\circ}$ (no porous area on the leading-edge flap).

Figure 11.- Chordwise pressure distributions for the model having the full-span 40° leading-edge flap and the 55° trailing-edge area-suction flap.

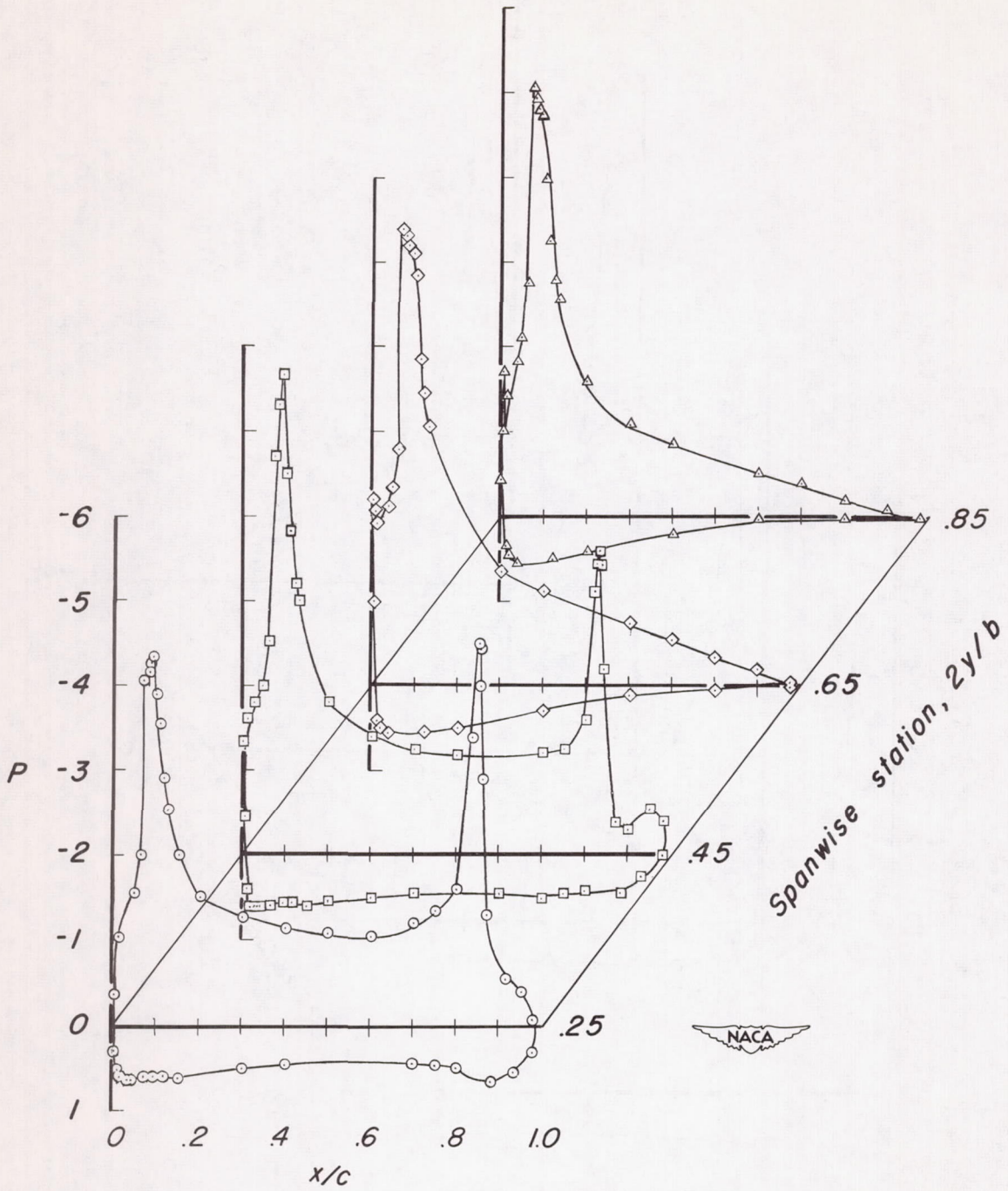

(b) $\alpha = 13.0^{\circ}$ (no porous area on the leading-edge flap).

Figure 11.- Continued.

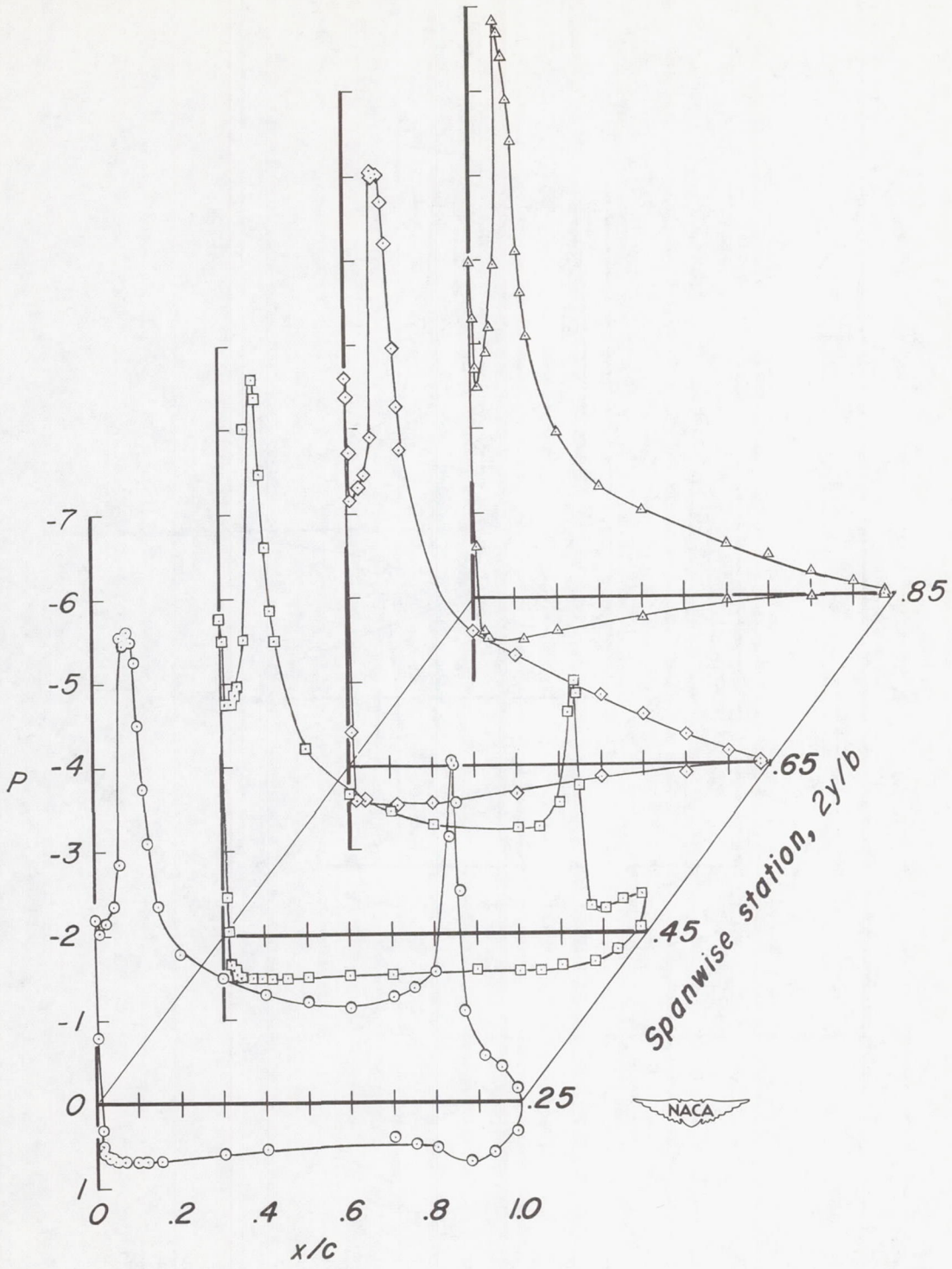

(c) $\alpha = 17.2^{\circ}$ (with area suction on the leading-edge flap).

Figure 11.- Continued.

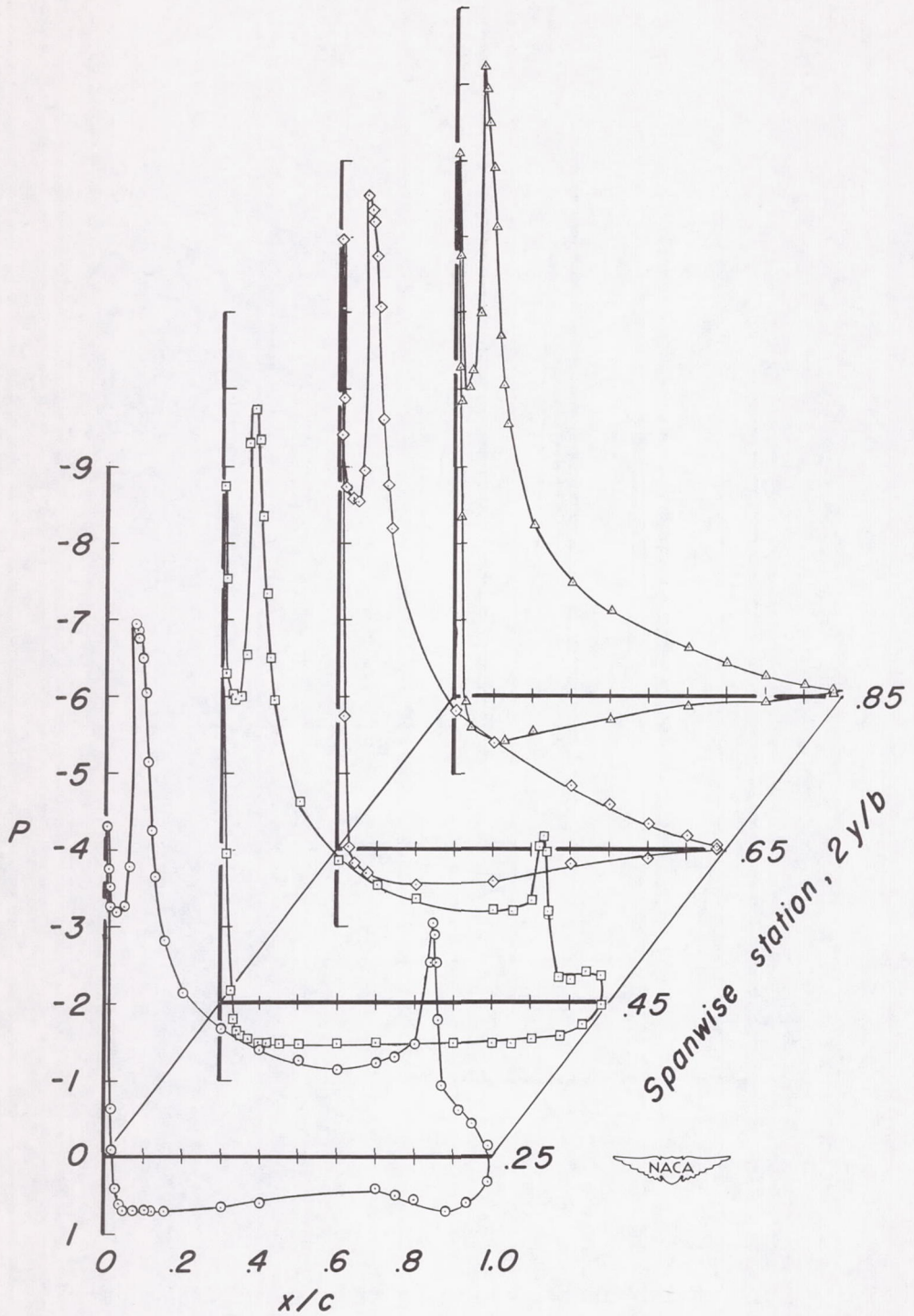

(d) $\alpha = 21.3^{\circ}$ (with area suction on the leading-edge flap).

Figure 11.- Continued.

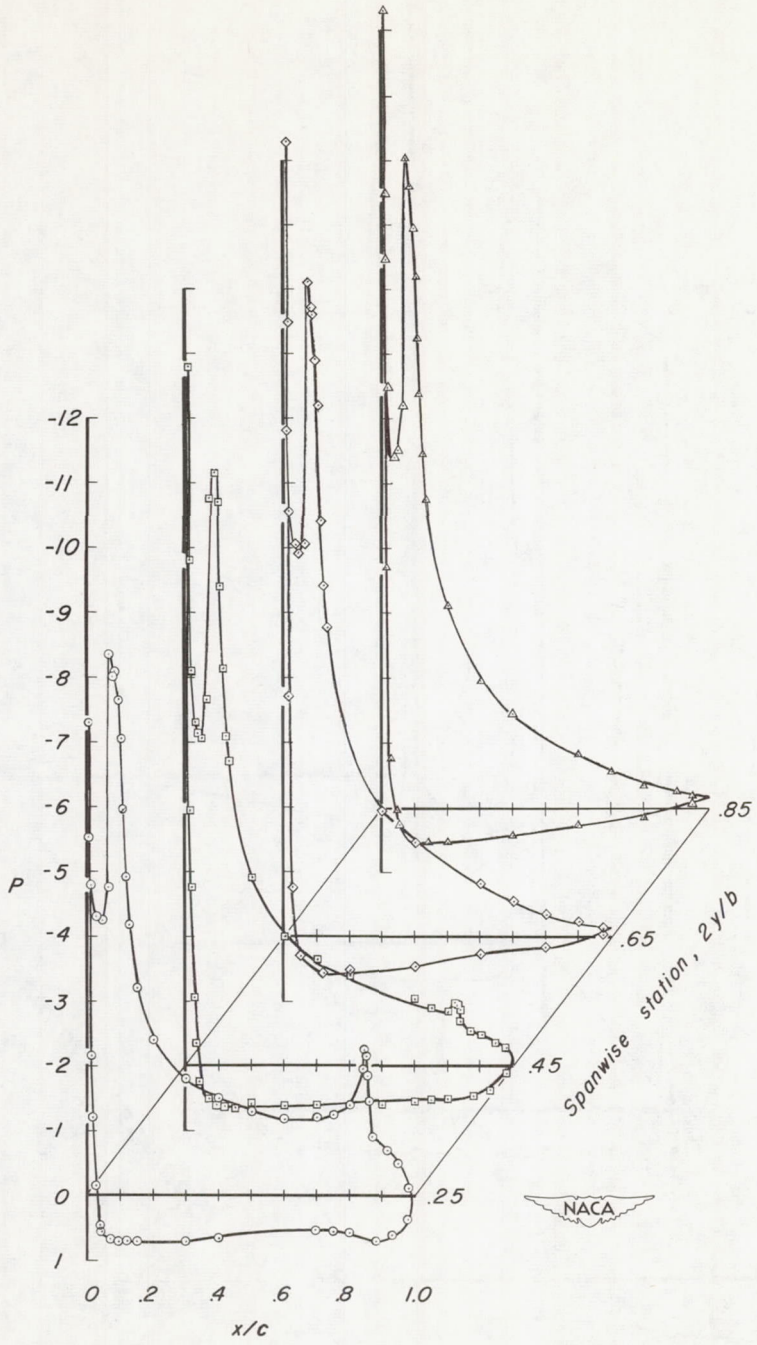

(e) $\alpha = 25.4^{\circ}$ (with area suction on the leading-edge flap).

Figure 11.- Continued.

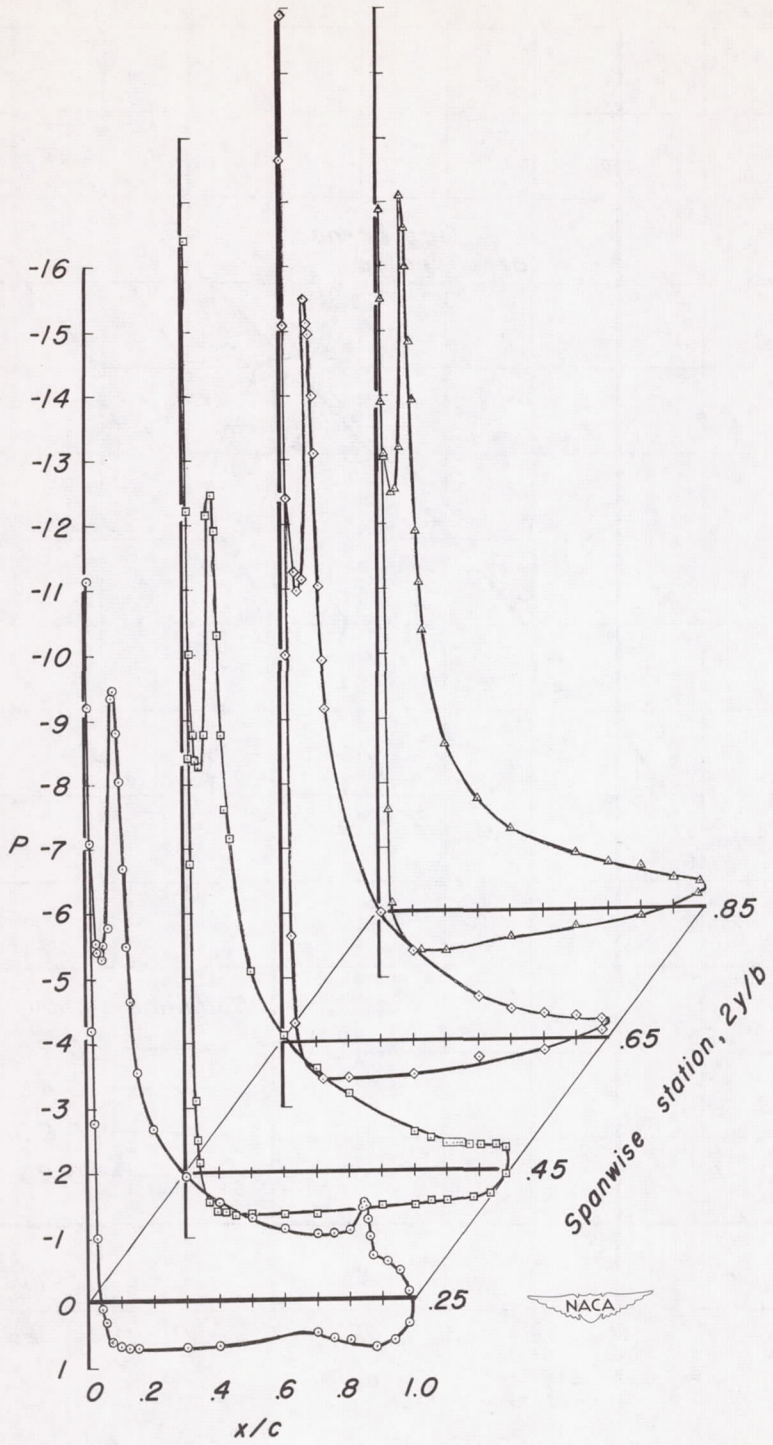

(f) $\alpha = 29.5^{\circ}$ (with area suction on the leading-edge flap).

Figure 11.- Concluded.

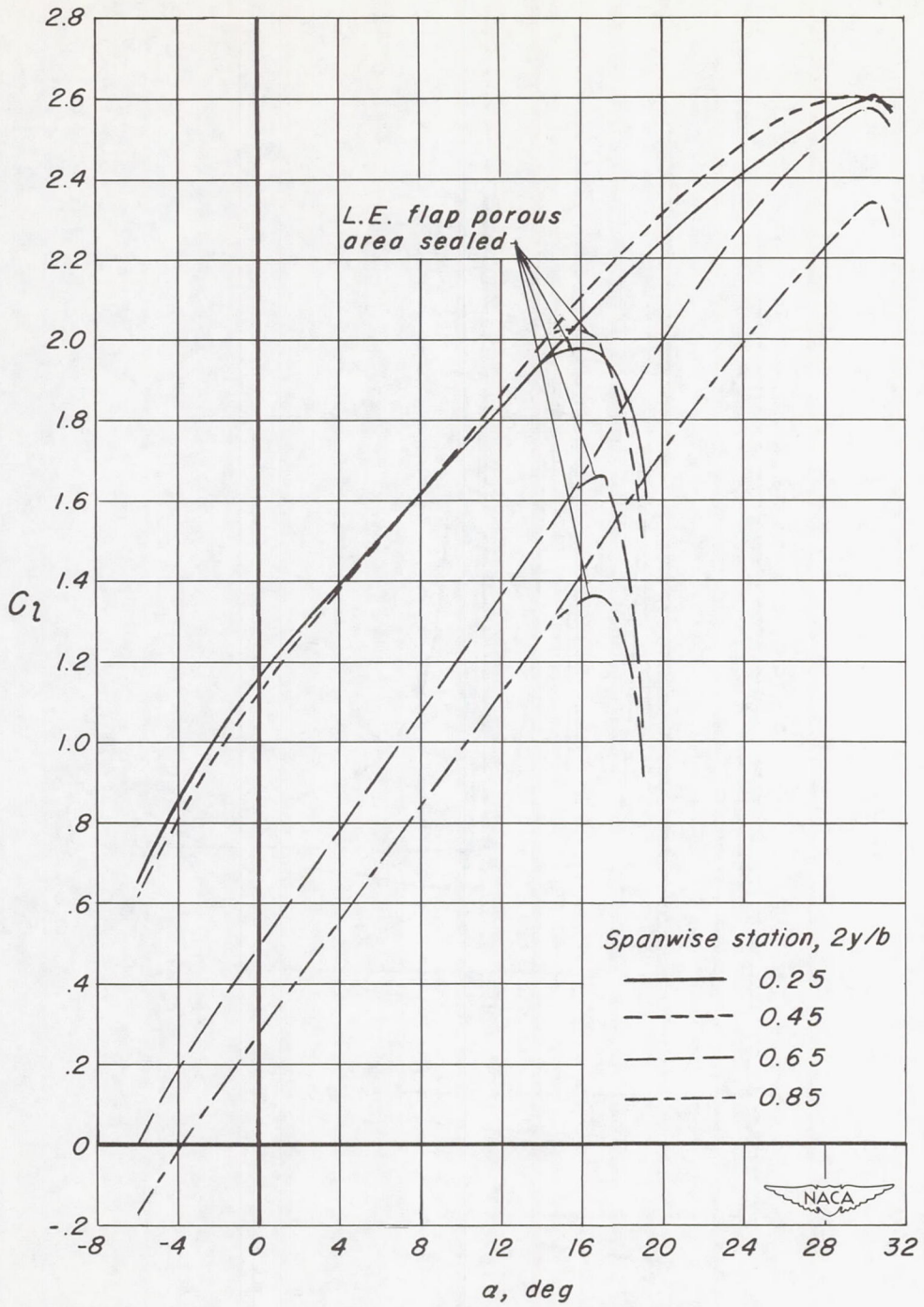

Figure 12.- Variation of section lift coefficients with angle of attack for the model with the 40° leading-edge area-suction flap and the 55° trailing-edge area-suction flap.

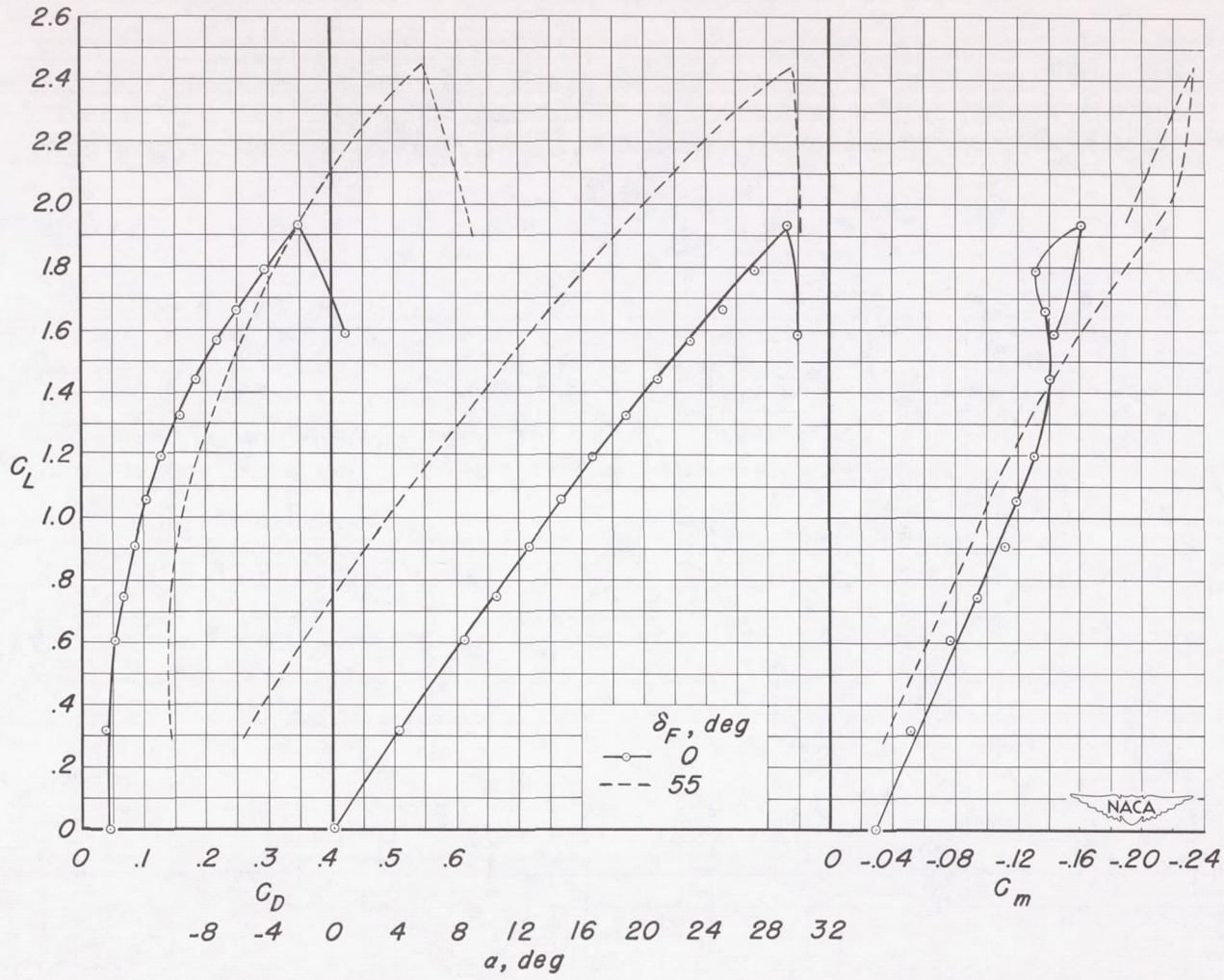

Figure 13.- Comparison of the aerodynamic characteristics of the model having an undeflected trailing-edge flap with those of the model having a 55° trailing-edge area-suction flap; 40° leading-edge area-suction flap; W/S = 40 pounds per square foot.

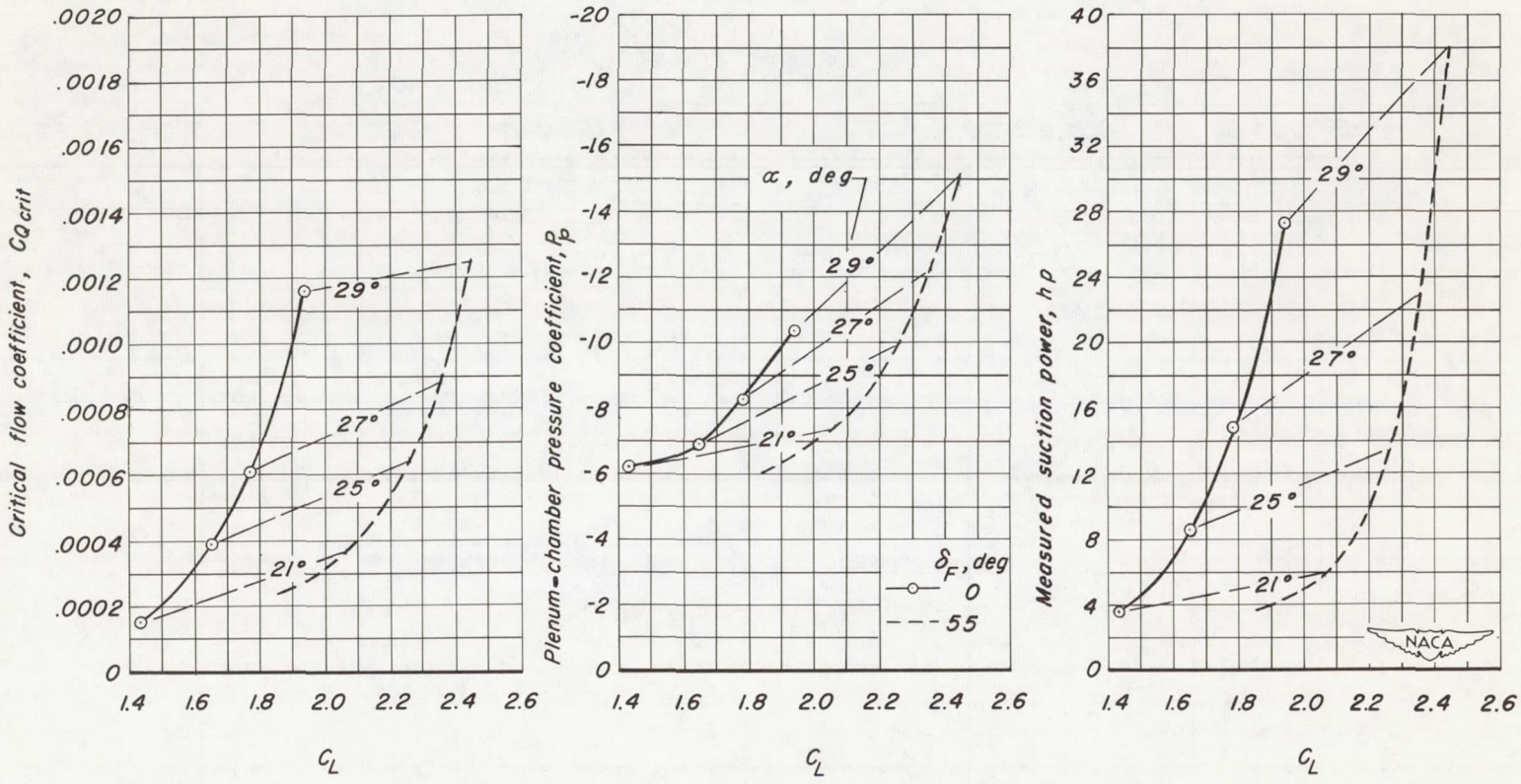

Figure 14.- Suction requirements for the 40° leading-edge area-suction flap with an undeflected trailing-edge flap and with a 55° trailing-edge area-suction flap; W/S = 40 pounds per square foot.

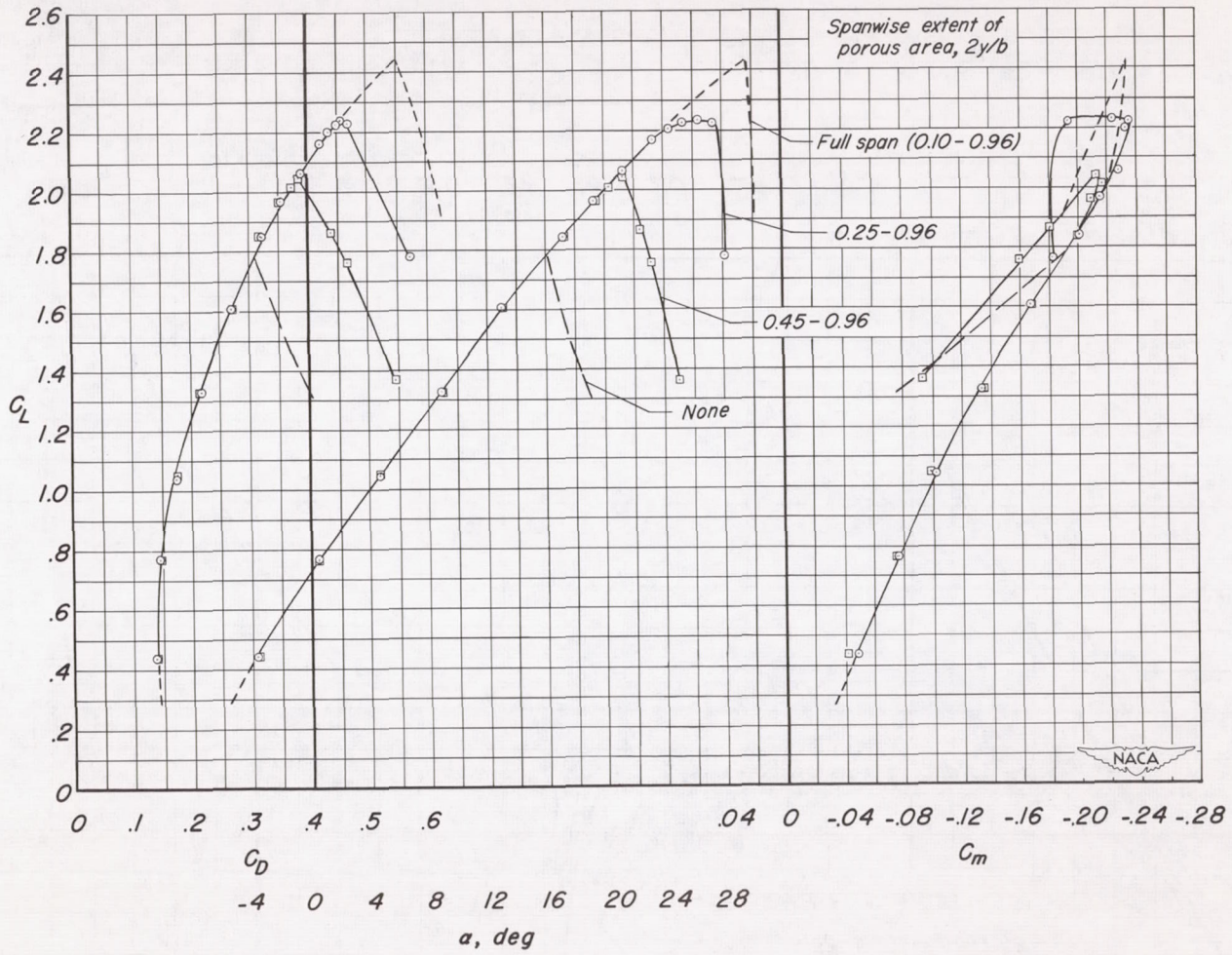

Figure 15.- Aerodynamic characteristics of model with partial-span area suction on full-span 40° leading-edge flap; chordwise porous-area configuration 1; 55° trailing-edge area-suction flap.

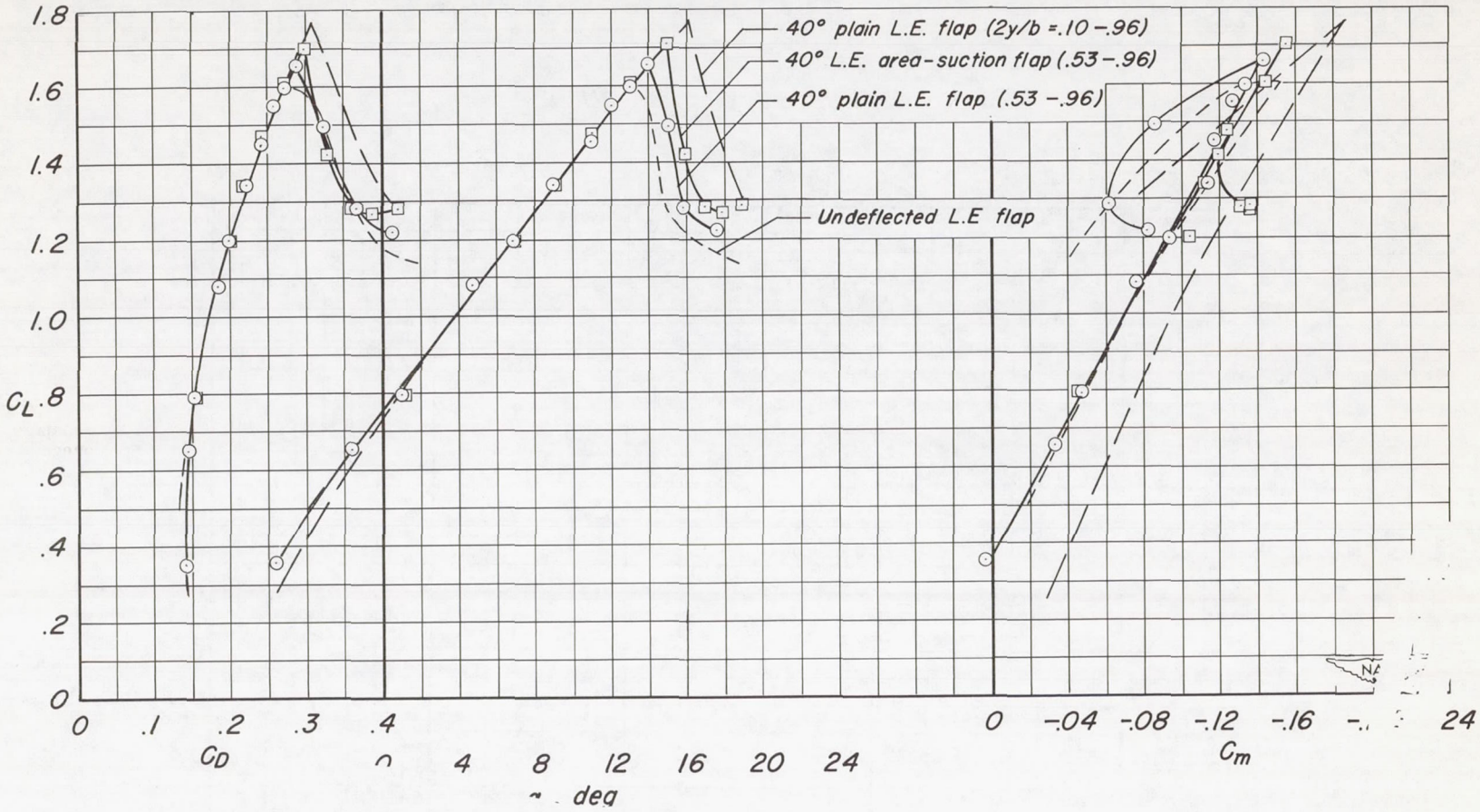

Figure 16.- Aerodynamic characteristics of model with various leading-edge flaps; 55° trailing-edge area-suction flap.